US.6
932A!

AIR FORCE research review

Number 3

May ★ December 1971

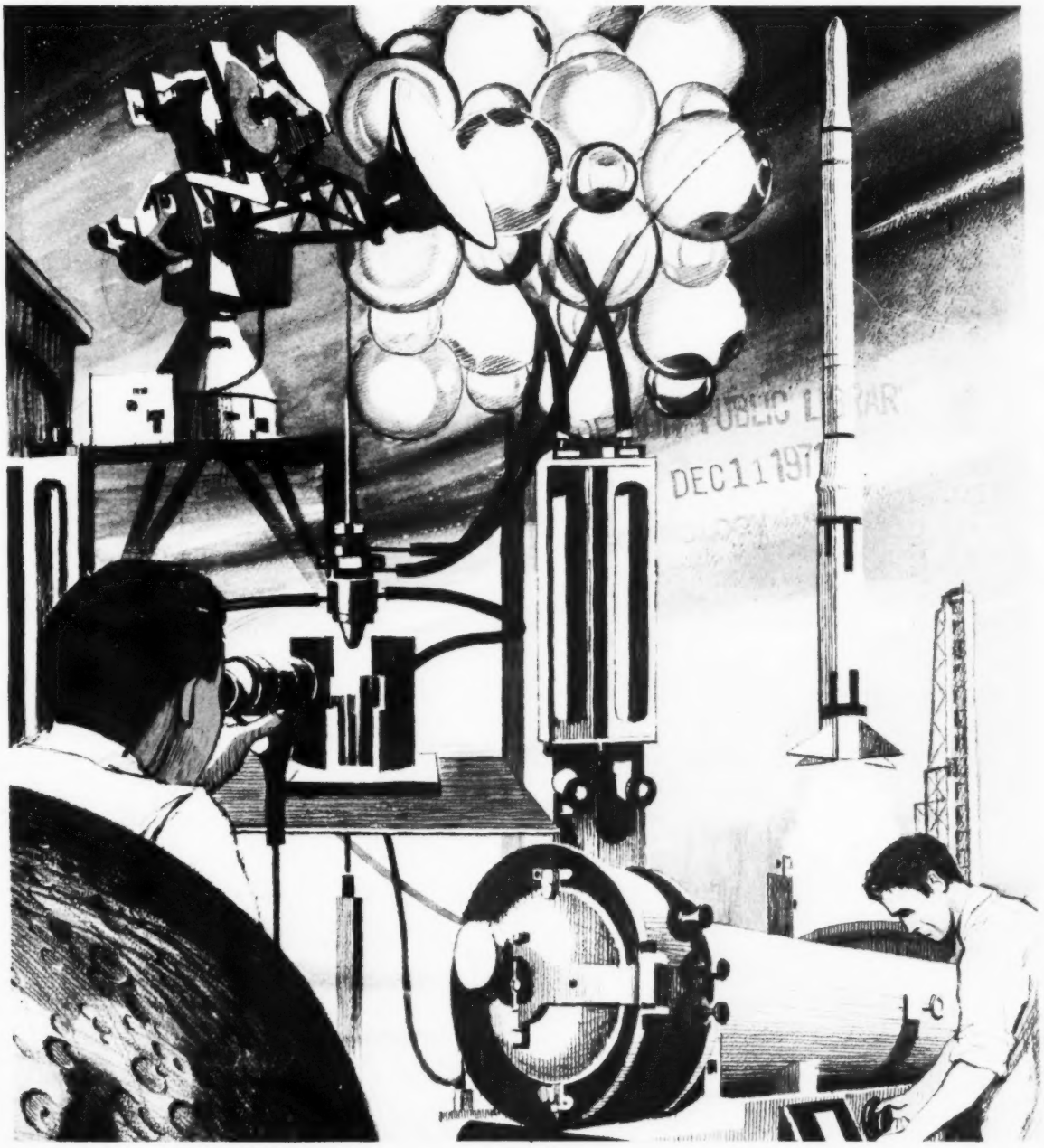

DEC 11 197

Air Force Systems Command

AFSCRP 80-2

Approved for public release; distribution unlimited.

AIR FORCE
research review

NUMBER 3

MAY ★ DECEMBER 1971

The Air Force Research Review is published bimonthly. To be considered for publication in a future issue, articles related to research should be submitted by AFSC laboratories to AFSC/DLLT/PUB, Andrews AFB, Washington, D.C. 20331. Questions or suggestions should be referred to the Editor, AUTOVON 858, Area Code 301, GIDC 185, Local Code 981, Extension 4634. The objective of this publication is to make the scientific community continually aware on a timely basis of unclassified research projects conducted and sponsored by the Air Force.

ETHEL GAMER, Editor

For sale by the Superintendent of Documents (Catalog No. D301.69/6-2), U.S. Government Printing Office, Washington, D.C. 20402: per year $2.00 domestic, $2.50 foreign, per single copy 35¢.

AFSCRP 80-2

Approved for public release; distribution unlimited.

NOTICE: To eliminate the publication date time lag caused by and continuing since the merger of OAR into AFSC in July 1970, this issue has been dated May-December 1971. As this issue will close out the calendar year 1971, an Index for 1971 has been included.

Table of Contents

REGULARIZABLE ILL-POSED PROBLEMS
Dr. David A. Lee
Applied Mathematics Research Laboratory, ARL 1

FLOW SEPARATION ON A SLENDER CONE AT ANGLE OF ATTACK
Kenneth F. Stetson
Fluid Dynamics Facilities Research Laboratory, ARL 4

ALUMINUM HIGH ENERGY DENSITY CONCENTRATION CELLS
Lt Colonel Lowell A. King and Major David W. Seegmiller
U.S. Air Force Academy
Captain Armand A. Fannin, Jr.
The Frank J. Seiler Research Laboratory 8

X-RAY PHOTOGRAPHS OF POWDER IN VORTEX FLOWS
Lt B.N. Turman
Energy Conversion Research Laboratory, ARL 12

INERTIAL NAVIGATION, GUIDANCE, AND CONTROL RESEARCH
Lt Colonel John Paul Hyde
Directorate of Aerospace-Mechanics, FJSRL 14

APPROXIMATION THEORY
Dr. O. Shisha
Applied Mathematics Research Laboratory, ARL 17

SCIENTIFIC NOTES

Oxidation of Titanium-Aluminum-Gallium Alloys
Metals and Ceramics Division, AFML 19

Fracture Mechanics of Fiber Reinforced Laminated Plastic Composites
Non-metallic Materials Division, AFML 19

Mass Spectrometric Determination of Volatile Electrode Products
Air Force Office of Scientific Research 20

Supersonic Turns Without Superbooms
Air Force Office of Scientific Research 20

Studies to Improve Radar Target Perception
Air Force Office of Scientific Research 20

Low Temperature Infrared Spectroscopy of Hydrogen Bonded Polymers
Materials Physics Division, AFML 20

Erosion Mechanisms of Graphite Materials
Materials Support Division, AFML 21

Compressive Behavior of Unidirectional Fiber Reinforced Plastic Composites
Nonmetallic Materials Division, AFML 21

New, Improved Shift Reagents for Simplifying NMR Spectra
Materials Physics Division, AFML 22

Yttrium Orthoaluminate—An Important New Laser Host Material
Materials Physics Division, AFML 22

READERS INTERCHANGE 24

INVENTION DISCLOSURES 24
Epoxy Resistance Thermometer 24
Method of Fabricating Lightweight Targets for Radar Measurements 24
Transfer Discharge Ion Getter Vacuum Pump 24
Deflection Modulation Display 24
Boundary Layer Probe 24
Improved NMR Probe for Magnetic Field Measurements 24
A Wideband, Low Noise Frequency Modulator That Can Be Used for Rapid Modulating Rates 24

RESEARCH ADVANCES 25
Exoatmospheric Infrared Calibration 25
Langmuir Probe Data Reduction Program 25
Effect of Unsymmetrical Nose-Bluntness on Stability Derivatives 25
Passive Optical Techniques for Space Object and Target Identification 25
New Centrifuge Test Method for Inertial Gyroscopes 26
Model for a Short-Range Dogfight Missile 26
The Ram-Wing: Theory and Experiment for Near-Surface Flight 26

RESEARCH NEEDS 27
State-of-Charge Level Sensing in Secondary Batteries 27
Boiling Phenomena Associated With Confined Spaces 27
MHD Lasers 28
Type II Superconductors and Their Applications 28
Fracture Mechanics—Crack Stoppers 28
Data Signaling Above Nyquist Rate 29
Area Ratio Ejectors as STOL High Lift and Propulsion Devices 29
Speech Digitization Techniques 30
Hundred Megabit to Gigabit Logic Study 30

1971 INDEX 31

REGULARIZABLE ILL-POSED PROBLEMS

DR. DAVID A. LEE
Applied Mathematics Research Laboratory, ARL

Over the last half-century the idea of a well-posed problem has been an important concept in applied mathematics. Roughly speaking, a problem is "well-posed in the sense of Hadamard" if it has a unique solution that depends continuously on its data. If a problem is not well-posed, then it cannot, according to the conventional point of view, be a useful model of a physical situation. For, if the problem does not have a solution–that is, if it is not logically consistent–then it certainly is not useful. A problem with two different solutions is not much help either. And if a problem has a unique solution that does not depend continuously on its data, it is of no practical use, since its solution cannot be determined from experimental data.

Recently this last point has been carefully re-examined because quite plausible and potentially useful problems, whose solutions do not depend continuously on their data, crop up fairly frequently. Such problems arise, for example, in a standard method for determining a polymer's molecular weight distribution, in attempts to infer the shapes and locations of underground deposits by mapping the local gravitational field, in attempts to determine the microfield in a plasma from spectroscopic observations, and in a great many experimental situations where the desired quantity f(x) cannot be observed directly but is "blurred" by some apparatus so that one obtains values for the function y(x) connected to f by an integral equation of the form

$$y(x) + \int_a^b k(x - z)\, f(z)dz$$

In each of these examples the problem is of the type called "regularizable ill-posed problems." The "ill-posedness" of such a problem has a special nature that allows one to give error estimates for approximate solutions. Experimental errors do, however, have different and potentially more damaging effects on approximate solution schemes for regularizable ill-posed problems than they do on solution schemes for well-posed problems. As we shall see, observational errors impose limits on the amount of fine detail that can be determined for the solutions of regularizable ill-posed problems.

A study of regularizable ill-posed problems, which has led to the development of useful error estimates for approximate solution schemes for molecular weight distributions (1) and for plasma microfields, is being carried out by Dr. David A. Lee of the ARL's Applied Mathematics Research Laboratory, in collaboration with Dr. M. Gehatia and Dr. Donald Wiff, AF Materials Laboratory, and with Dr. Jorgen Birkeland of ARL's Plasma Physics Research Laboratory.

A simple regularizable ill-posed problem, which displays many features of the class and which has a fairly plausible physical origin, is the following: Suppose one tries to determine the weight distribution of a non-uniform string by hanging it from two supports that are at equal elevations, measuring the tension in the cord, and then observing its displacement under gravity. In an appropriate system of units, for small displacements, the unknown weight distribution w(x) is connected to the displacement y(x) by the equation

$$w(x) = \frac{d^2 x}{dx^2} \qquad 0 \leqslant x \leqslant 1 \qquad (1)$$

Now suppose that in a certain case

$$y(x) = x(1 - x)(x^2 - x - 1) \equiv y_0(x) \qquad (2)$$

Then from (1),

$$w(x) = 12x(1 - x) \equiv w_0(x) \qquad (3)$$

But consider the case

$$y(x) = x(1 - x)(x^2 - x - 1) + \epsilon \sin(k\pi x) \equiv y_1(x) \qquad (4)$$

where k is an integer.
Again using (1), one finds

$$w(x) = 12x(1 - x) - k^2 \pi^2 \epsilon \sin(k\pi x) \equiv w_1(x) \qquad (5)$$

Now, while the largest difference between y_0 and y_1 is ϵ, w_0 and w_1 differ by as much as $k^2 \pi^2 \epsilon$. Clearly, very small differences in the observed displacement can lead to very big differences in the inferred weight distribution w and that is the essence of the ill-posedness of this problem. (Incidentally, if k is even, w_0 and w_1 both correspond to exactly the same total loading of the string, 2 units.)

Now a practical man, looking at this example, is likely to observe that the difference between y_1 and y_0 is $\epsilon \sin$

$(k\pi x)$, a function which oscillates rapidly for large k, and that it is in fact these oscillations that lead to the big differences between w_0 and w_1. He may then conclude that the way out of trouble is to use his measurements to approximate y(x) in such a way that rapid oscillations cannot be produced. The possibility of overlooking such oscillations will not worry him very much, because "they are not physical".

Indeed, these ideas are useful. One could, for instance, use measurements to determine the first few terms in a series for y of the form

$$y(x) = \sum_{1}^{\infty} c_n \sin(n\pi x) \tag{6}$$

Representation (6) for y leads, formally, to

$$w(x) = \sum_{1}^{\infty} (-n^2\pi^2 c_n) \sin(n\pi x) \tag{7}$$

and, if we agree to limit ourselves to cases for which w(x) is a continuous function vanishing at 0 and at 1, the series (7) does in fact converge to w(x). If, following practical ideas, one then truncates series (6) and (7) after M terms, he will obtain an approximate solution of the problem (2), call it $w_M(x)$, given by

$$w_M(x) = \sum_{1}^{M} (-n^2\pi^2 c_n) \sin(n\pi x) \tag{8}$$

Experience will show that, if M is kept small (on the order of 2 or 3), in many cases very reasonable answers are produced by approximation (8). In particular, observational errors do not lead to erratic behavior of the approximate solution.

At this point, though, even our practical man would probably like to know something about the accuracy of his proceedings. He would almost certainly appreciate some guidance for the choice of the order of approximation M. As it happens, discussion of these questions leads to some interesting results.

Suppose that the measurements have some error. That is, suppose that the observations yield not y(x), but

$$\tilde{y}(x) \equiv y(x) + e(x) \tag{9}$$

where we will assume that e(x) is some piecewise continuous function on [0,1].

Let the error E(x) of scheme (8) be defined as the difference between w(x) and the result of applying scheme (8) to $\tilde{y}(x)$. It can be shown that

$$\|E(x)\|^2 \leq \tfrac{1}{2} \sum_{M+1}^{\infty} n^4\pi^4 c_n^2 + (M^4\pi^4/2)\,\|e(x)\|^2 \tag{10}$$

where $\|f(x)\|$, measure of the "size" of the function f(x) on [0,1], is defined as

$$\|f(x)\|^2 = \int_0^1 f^2(x)dx$$

Now, inequality (10) reveals the nature of the error of (9) pretty clearly. For every w(x) in the class we are considering, the sum

$$\sum_{1}^{\infty} n^4\pi^4 c_n^2 = 2\|w(x)\|^2$$

converges. Therefore the sum in (10) can be made as small as one pleases simply by choosing M sufficiently large. But the second term in (10) increases with M. Thus the error bound, being the sum of a decreasing function and an increasing function, has a minimum value for some M. That is, there is an optimum M. If one works with a smaller M than the optimum, he may be neglecting potentially recoverable information. If he uses a larger M than the optimum, he will not necessarily improve his results and may in fact degrade them.

Also, the behavior of the sum in (10) is fixed by w. It follows that the value of the optimum M generally decreases as $\|e\|$ increases. Now, the small-scale details of w(x) are described by the higher-order terms—those for larger n—in series (7). Since the largest n that can be successfully treated by the approximate inversion scheme typically decreases with increasing $\|e\|$, one sees that observational errors limit the resolution attainable with approximate solution scheme (8) for the present regularizable ill-posed problem. Analogous error bounds for approximate solution schemes applied to well-posed problems contain only terms like the sum in (10), which can be made arbitrarily small by taking M sufficiently large.

In figure 1, the ratio of the error bound (10) to $\|w_0\|$ is plotted against M for various values of $\|e\|/\|y_0\|$. A similar curve is shown in figure 2 for the plasma microfield problem. In this case, k denotes the limit of a truncated Fourier integral for the unknown microfield.

The main features of the example given above are generally found for regularizable ill-posed problems: experimental errors introduce resolution limits, and there is an optimum order of approximation for a given approximate solution scheme. It is important to realize this in order to avoid either wasting information or attempting to infer details that cannot actually be determined from the experiment at hand.

Dr. David A. Lee has been a Research Mathematician in the Applied Mathematics Research Laboratory at ARL since July 1963. Currently, he is studying certain regularizable ill-posed problems that appear in physical contexts.

Dr. Lee earned the B.S. in Electrical Engineering at the University of Missouri in 1959. Studying with both Danforth and Woodrow Wilson Fellowships, he received an Sc.M. degree in Applied Mathematics from Brown University in 1961. In 1963 the Illinois Institute of Technology awarded him a Ph.D. in Mechanics.

Articles on Dr. Lee's research on applications of analysis to problems in turbulence and plasma theory has appeared in a number of leading scientific journals. Recently, his work on the determination of molecular weight distribution appeared in the Journal of Polymer Chemistry.

REFERENCE

(1) D.A. Lee, "On the Determination of Molecular Weight Distributions From Sedimentation-Diffusion Equilibrium Data at a Single Rotor Speed," *J. Polymer Sci.* Part A-2, Vol. 8 (1970), 1039-1056.

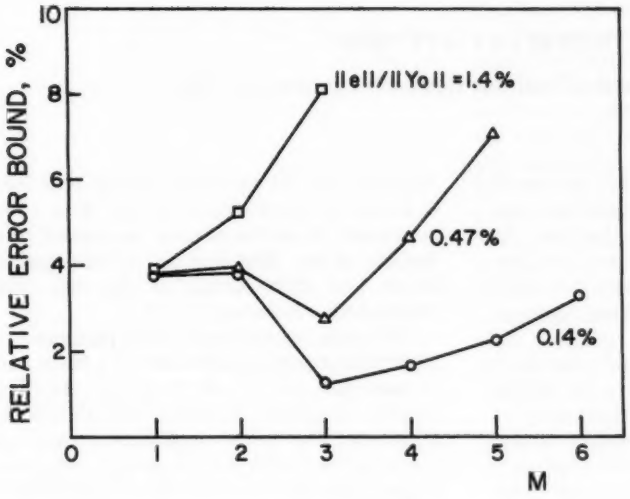

Figure 1. Variation of the bound on relative error of scheme (8) with order of approximation and error norm.

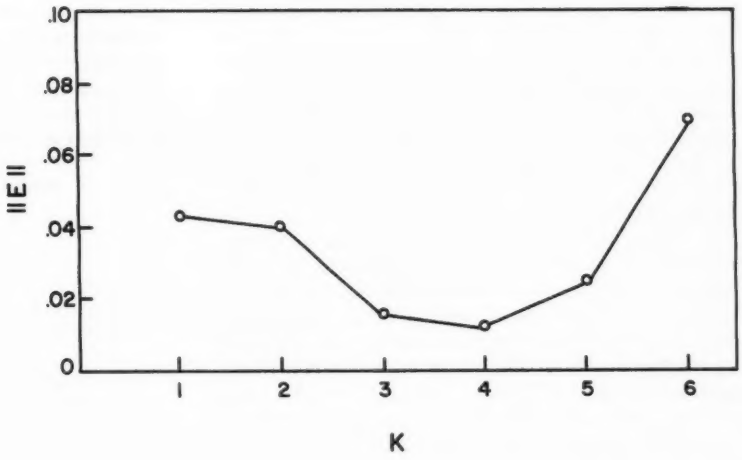

Figure 2. Variation of error estimate for plasma microfield problem with truncation wave number.

Flow Separation on a Slender Cone at Angle of Attack

KENNETH F. STETSON

Fluid Dynamics Facilities Research Laboratory, ARL

Vehicle design and performance studies require knowledge of the fluid flow about the vehicle and the interactions of various components of the vehicle with this flow. To develop adequate analytical techniques for such calculations, it is necessary to define an appropriate flow field model that contains the basic features and characteristics of the fluid flow.

The definition of a suitable flow field model may have varying degrees of complexity, depending upon the vehicle configuration, its attitude, its velocity, the flight environment, and the amount of sophistication desired in the calculations. Even a very simple configuration, such as a cone, can produce an extremely complex flow field structure containing three-dimensional flow and viscous-inviscid interactions.

One of the least understood features of a flow field is associated with separated flow.* Separated flows associated with base regions, flaps, flares, control surfaces, and shock inpingement have received so much attention in recent years that considerable knowledge has been acquired about these flow situations. However, the separated flow about the leeward side of a vehicle at angle of attack is a complicated three-dimensional flow problem which has not been amenable to solution. Only limited details are available on such flows.

The three-dimensional separation bubble, as shown schematically in figure 1, has been considered by many investigators to be the most likely flow field model for separation on a blunt cone at angle of attack. Significant features of this model are a separation line which originates from a singular point (a point on the vehicle surface where all components of skin friction are zero) on the most leeward ray, and a separated layer enclosing a "bubble". The separation bubble is fed by low energy fluid traveling forward from the base region. Control surfaces located within the separation bubble would then be ineffective. Because the results of the present investigation clearly indicated that the separation bubble flow field model was an incorrect representation of these data, a new model for hypersonic three-dimensional separation was proposed. Samples of the data that led to this conclusion will be shown and more details of this investigation can be obtained from References 1 and 2.

Recently experiments were performed in the ARL 20-inch hypersonic wind tunnel at a Mach number of 14.2 to investigate the flow resulting from the complex viscous-inviscid interactions associated with a slender body at angle of attack. The model used was a sting-mounted, 5.6° half-angle cone with three nose tip configurations: a sharp tip and nose radii equal to 10% and 30% of the base radius. Cone surface pressures, pitot pressure surveys, and surface oil flow patterns were obtained for angles of attack up to 18°. Surface pressure measurements show the adverse pressure gradients that were produced by viscous-inviscid interactions when the cone model was at angle of attack. Adverse pressure gradients produce a resistance to the flow that may turn the fluid; if the pressure changes are severe enough, they can induce the fluid to separate from the model surface.

SEPARATED FLOW FIELD MODEL

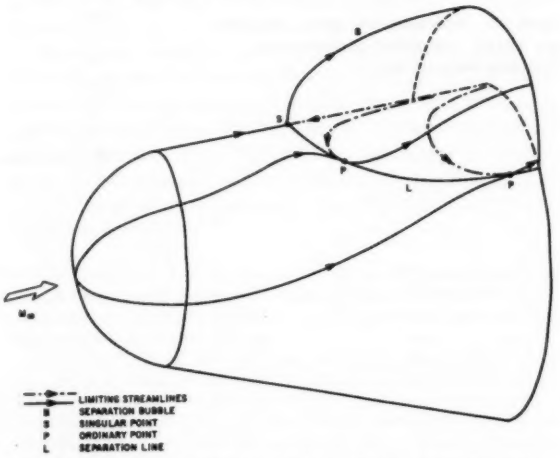

Figure 1. Separation bubble flow field model for three-dimensional separation.

**Separated flow is the condition where fluid that has been traveling along the vehicle surface breaks away, or separates, from the surface. Separated flow may result from an abrupt change in surface direction, such as at the base of the vehicle or at a cavity in the surface. However, a common occurrence of flow separation is related to an adverse pressure gradient (an increasing pressure) produced by such situations as the protuberance of a flap, control surface, or flare; by the impingement of a shock wave; or by viscous-inviscid interactions on the leeward (sheltered) side of a vehicle at angle of attack.*

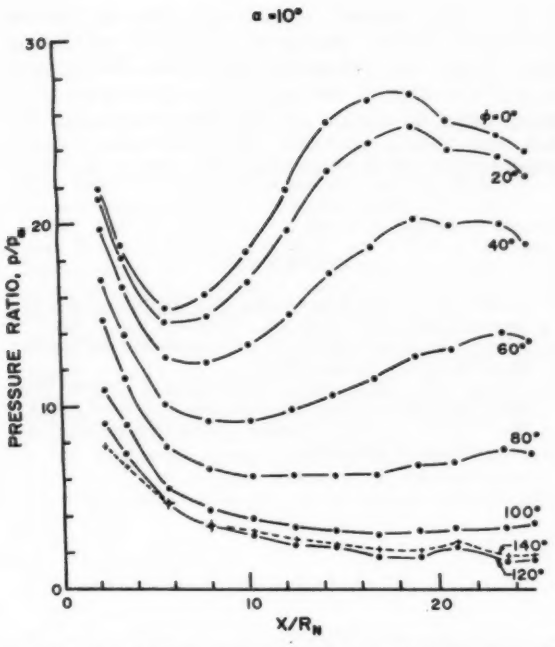

Figure 2. Longitudinal pressure distributions, 30% bluntness, 10° angle of attack.

Figure 2 shows the pressure distribution along several rays of the blunt cone at a 10° angle of attack. In this and subsequent figures,

X = the distance along the cone surface from the zero angle of attack stagnation point

R_N = nose radius

X/R_N = distance behind the blunt nose

ϕ = cone circumferential angle, measured in a clockwise direction, based on a head-on view, with the most windward ray designated as $\phi = 0$

Significant features are the large favorable pressure gradients (expanding flow) near the nose tip and overexpansion and subsequent recompression on the windward side. The recompression on the windward side does not cause the fluid to separate from the surface, but accentuates the turning of the flow around the cone.

Figure 3 is an example of the circumferential pressure distributions obtained on a blunt cone. At small X/R_N's, the boundary layer is attached and the minimum circumferential pressure occurs on the most leeward ray (ϕ = 180°). At larger X/R_N's, two symmetrical minimum pressure locations occur off the leeward plane of symmetry, followed by adverse pressure gradients in the cross flow plane. The points shown on the curves are separation line locations obtained from oil flow photographs. With increasing angle of attack, the origin of separation occurs closer to the nose tip.

The surface oil flow technique was found to be a simple and easy method for obtaining three-dimensional separation data. Since the skin friction force produced by the fluid flow causes the oil to flow along the model surface, the oil patterns produced indicate skin friction lines or surface streamlines.

Figure 4 is an example of oil flow results for the cone with 30% bluntness at a 10° angle of attack. Oil was applied with a brush to the windward region and the nose cap. The oil from the windward region was observed to flow around the cone and turn toward the rear of the cone as it approached the adverse pressure gradient and the separation line. At the separation line, the oil accumulated and then traveled down the separation line to the rear of the cone. Since the boundary layer separated from the cone surface at this line, no oil was carried into the separated flow region. From the oil flow tests, it was determined that the separation line did not originate from a singular point, but from a region where only the lateral component of skin friction was zero. There was no evidence of reverse flow in the separated region.

A number of pitot pressure surveys were made of the leeward region to obtain general information about the

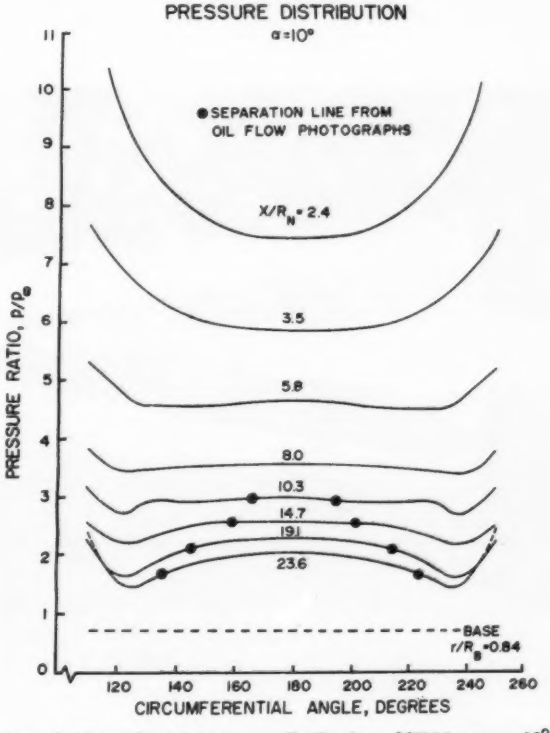

Figure 3. Circumferential pressure distributions, 30% bluntness, 10° angle of attack.

flow field. Figure 5 is an example of the pitot pressure contour maps obtained from these surveys. By assuming a constant static presure in the separated region, it was possible to make approximate calculations of local Mach number. Throughout the region of the twin vortex system associated with the separated flow, the flow was found to be supersonic, thus substantiating the concept of a supersonic vortex with this type of separation.

Based on the results of this investigation, a new model for hypersonic three-dimensional separation was proposed. This model contains symmetrical supersonic helical vortices with an attachment line on the most leeward ray. The vortices are in contact with the surface (at least up to an 18° angle of attack) and no subsonic reverse flow or singular points are associated with the vortex pattern. Figure 6 is a conceptual drawing of this model of separation on a slender blunt cone at angle of attack, using "stream ribbons" to illustrate the vortex flow. This flow separation model is more adaptable to analytical treatment than the "separation bubble" concept and, hopefully, will aid in future design and performance calculations. The areas of aerodynamic controls and aerodynamic heating are interesting topics for further investigations because this new flow field model infers better control effectiveness in the leeward region and more severe aerodynamic heating.

REFERENCES

(1) Stetson, K.F., and E.S. Ojdana, Jr., "Hypersonic Laminar Boundary-Layer Separation on a Slender Cone at Angle of Attack," *American Institute of Aeronautics and Astronautics, Paper No. 71-129*, January 1971.

(2) Stetson, K.F., "Experimental Investigation of Laminar Boundary-Layer Separation on a Slender Cone at Angle of Attack at $M_\infty = 14.2$," *Aerospace Research Laboratories Report 71-xx*, June 1971 (to be published).

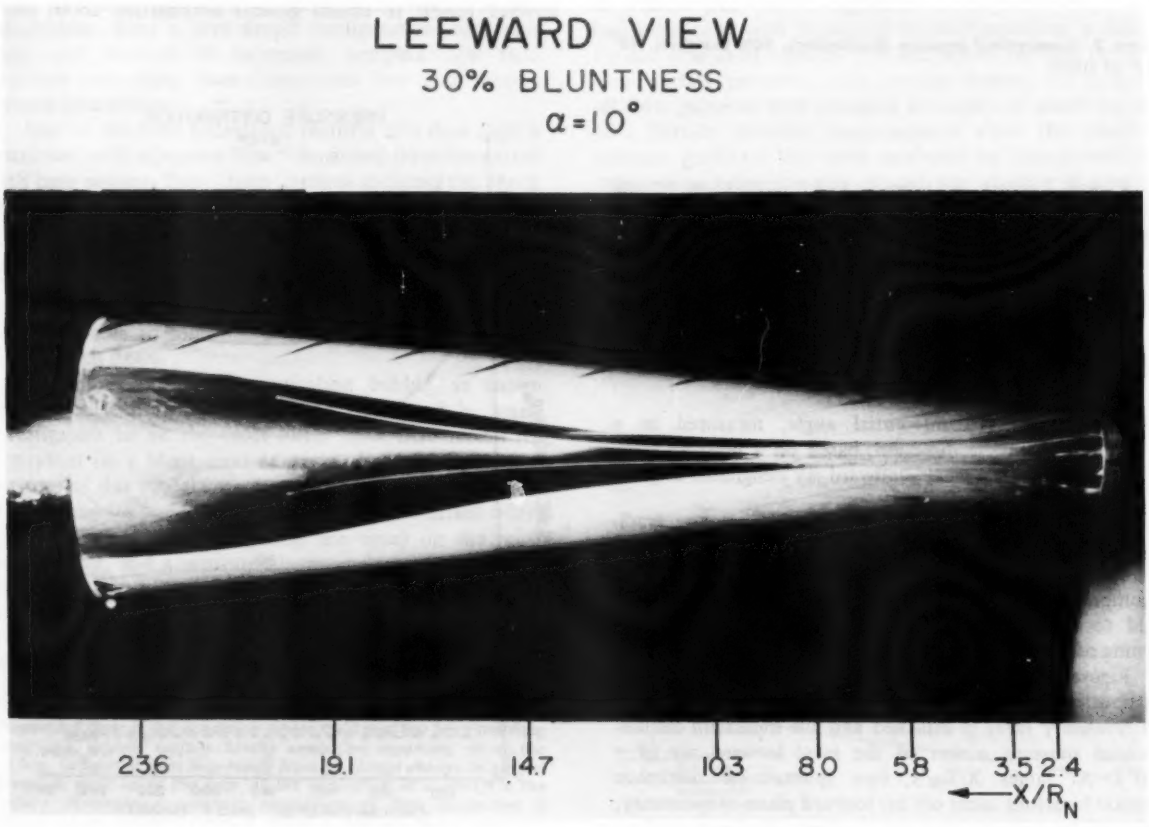

Figure 4. Oil flow photograph, leeward view, 30% bluntness, 10° angle of attack.

Kenneth F. Stetson has been a Group Leader in the Fluid Dynamics Facilities Research Laboratory at ARL since August 1969. His current research concerns the determination of limits of flight conditions that can be duplicated in ground test facilities and the scale effects required for the interpretation of the results.

Mr Stetson received a B.S. degree in Engineering Physics in 1949 from the University of Maine and a M.S. in Aeronautical Engineering in 1956 from the Ohio State University. He also graduated from the Air Force Institute of Technology, in 1952, after his recall to active duty in the Air Force in 1950.

Following Air Force assignments (1950-1956) in the Wind Tunnel Branch of the Aircraft Laboratory and the Fluid Dynamics Branch of ARL, he was employed by the Avco Corporation (1956-1968), concentrating on various aspects of the missile reentry problem. In August 1968 he returned to ARL for a year as a visiting Research Associate of Ohio State University.

Mr. Stetson has regularly published the results of his research since 1958, is an Associate Fellow in the American Institute of Aeronautics and Astronautics, and is listed in American Men of Science.

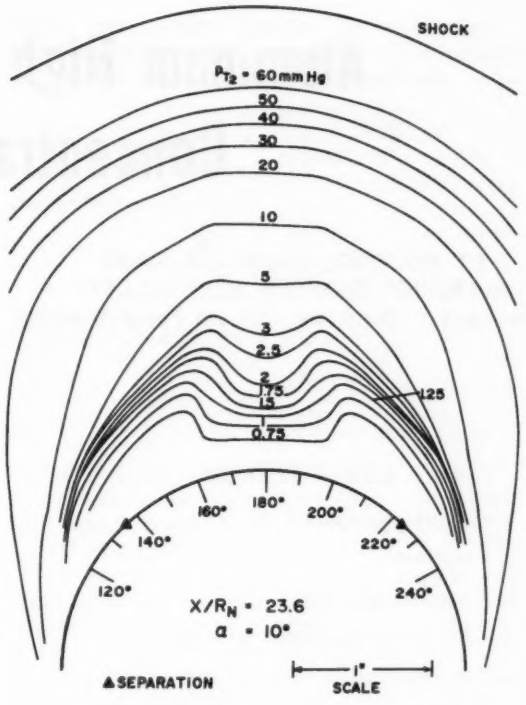

Figure 5. Blunt cone pitot pressure contours, X/R_N = 23.6, 10° angle of attack.

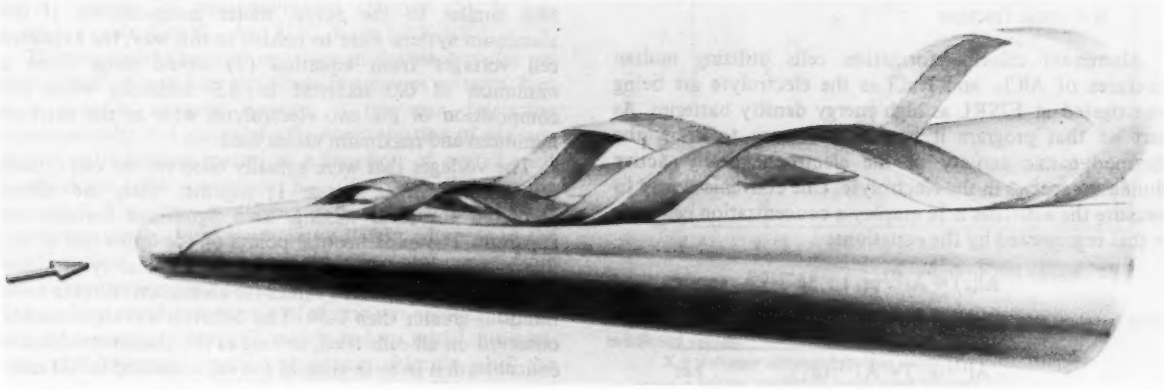

Figure 6. Conceptual drawing of new model of boundary-layer separation on a blunt cone at angle of attack.

Aluminum High Energy Density Concentration Cells

LT. COLONEL LOWELL A. KING
and MAJOR DAVID W. SEEGMILLER
Department of Chemistry, U.S. Air Force Academy

and CAPTAIN ARMAND A. FANNIN, JR.
The Frank J. Seiler Research Laboratory

LIST OF SYMBOLS

a = thermodynamic activity

$\underset{\sim}{e}^-$ = electron

ln = natural logarithm

n = number of equivalents per mole

s = solid

Al^{III} = electrochemically active species of aluminum in 3+ oxidation state

$\mathcal{E}$ = electromotive force

$\mathcal{F}$ = the faraday constant

K_i = equilibrium constant for the ith chemical reaction

N = apparent mole fraction $AlCl_3$ (the overall mole fraction of aluminum chloride in the $AlCl_3$-NaCl electrolyte)

R = universal gas constant

T = temperature in degrees Kelvin

X = mole fraction

Aluminum chlorine formation cells utilizing molten mixtures of $AlCl_3$ and NaCl as the electrolyte are being investigated at FJSRL as high energy density batteries. As part of that program it became necessary to know the thermodynamic activity of the electrochemically active aluminum species in the electrolyte. One convenient way to measure the activities is to employ a concentration cell such as that represented by the equations:

$$Al(s) \rightleftharpoons Al^{III}(a_1) + 3\underset{\sim}{e}^- \qquad \text{anode}$$

$$Al^{III}(a_2) + 3\underset{\sim}{e}^- \rightleftharpoons Al(\underset{\sim}{e}) \qquad \text{cathode}$$

$$Al^{III}(a_2) \rightleftharpoons Al^{III}(a_1) \qquad \text{net}$$

where the activities of aluminum and the observed cell voltage are related by:

$$\mathcal{E} = -\frac{RT}{n\mathcal{F}} \ln \frac{a_1}{a_2} \qquad (1)$$

Experiments

Concentration cells of a variety of designs were built. All had in common an aluminum wire immersed in each of two different electrolytes contained in separate electrolyte compartments. The electrolyte compartments were connected by a porous barrier to permit ionic flow between the two melts. Glass frits, asbestos wicks, Fiberglass mats, and very thin Pyrex membranes (which are conductive to sodium ions) were used as porous barriers in various experiments. Electrolytes were molten mixtures of aluminum chloride and sodium chloride, with the aluminum chloride content ranging from 0.498 mole fraction to 0.707 mole fraction. In practice, the composition of one electrolyte in a particular cell was held constant and the composition of the other electrolyte was changed by addition of crystals of $AlCl_3$ or NaCl.

The cell voltages calculated from equation (1) will yield the ratio of activities of aluminum in the two electrolytes. Many binary molten halide systems are reported to behave very nearly as ideal solutions, with thermodynamic activities similar to the actual molar compositions. If the aluminum system were to behave in this way, the expected cell voltages from equation (1) would range from a minimum of 0.0 millivolt to 4.5 millivolts when the composition of the two electrolytes were at the extreme minimum and maximum values used.

The voltages that were actually observed on one typical cell are shown in figure 1, together with the values predicted for ideal mixing. Two significant features are apparent. The experimental points on the upper half of the figure span over 0.2 volt, and are approximately 50 times larger than the predicted values for aluminum chloride mole fractions greater than 0.54. This behavior was reproducibly observed on all cells tried, so long as the aluminum chloride concentration in both arms of the cell exceeded 0.500 mole fraction. The other notable feature of these cells is the voltage increment of approximately 0.4 volt in addition to the previously cited unusually high voltage, whenever the

composition of aluminum chloride in one of the compartments was reduced to below 0.500 mole fraction. This increment also was reproducibly obtained.

Results

We decided to study the structure of the electrolyte, and particularly to determine the chemical fate of oxidized aluminum in these electrolytes, in order to answer such questions as: (1) Is the very high concentration cell voltage real, or an artifact? (2) Can the voltage be maintained in a battery over a reasonable depth of discharge? (3) Can this performance be improved upon? (4) Can this type of behavior be predicted for other concentration cell systems than an aluminum-based one? It is reasonably clear that all four questions can be answered affirmatively.

The following species have been postulated (1) to exist in aluminum-chloride/sodium-chloride melts:

$AlCl_3$	$AlCl_4^-$	Na^+
Al_2Cl_6	$Al_2Cl_7^-$	Cl^-
	$Al_3Cl_{10}^-$	

A reasonable set of reactions linking these anions and molecular species is given below. The indicated equilibrium constants relate to the equations as shown.

$$\left.\begin{aligned} 2AlCl_3 &\rightleftharpoons Al_2Cl_6 && K_0 \\ Cl^- + AlCl_3 &\rightleftharpoons AlCl_4^- && K_1 \\ AlCl_4^- + AlCl_3 &\rightleftharpoons Al_2Cl_7^- && K_2 \\ Al_2Cl_7^- + AlCl_3 &\rightleftharpoons Al_3Cl_{10}^- && K_3 \end{aligned}\right\} \quad (2)$$

It has been well established (2) that aluminum chloride in the vapor phase exists almost exclusively as the dimer Al_2Cl_6 at temperatures below 400°C. From the JANAF tables (3), one may calculate the vapor dimerization constant. Using this value and the ratio of aluminum chloride vapor pressure over $AlCl_3$-NaCl melts (4) to the vapor pressure of pure aluminum chloride (5), it was possible to calculate K_0. At 175°C, $K_0 = 2.9 \times 10^7$.

The proposed chemical reactions in the electrolytes are reminiscent of acid-base equilibria in aqueous systems. Just as is true in aqueous systems, if one can determine experimentally and accurately the concentration of any one of the participating species as a function of overall melt composition, the constants K_1, K_2, and K_3 can be evaluated. The only qualifying experimental data in the important composition range immediately adjacent to the 0.500 mole fraction aluminum-chloride point comes from the concentration cell work of Torsi and Mamantov (6). They added small increments of aluminum chloride to one arm of a concentration cell, which had an initial composition of 0.498 mole fraction aluminum chloride, until the composition reached 0.503 mole fraction. Their experimental cell voltages displayed typical titration curve behavior when plotted vs. composition. The titration data may be treated with the equilibrium expression.

$$K = \frac{K_2}{K_1} = \frac{{}^{X}Cl^- \; {}^{X}Al_2Cl_7^-}{({}^{X}AlCl_4^-)^2} \quad (3)$$

and the Nernst equation

$$\mathcal{E} = \frac{4RT}{3\mathcal{F}} \ln\left(\frac{{}^{X}Cl^-}{{}^{X}Cl^-_{\text{reference}}}\right) \quad (4)$$

At the equivalence point

$$\frac{K_2}{K_1} = \frac{({}^{X}Cl^-)^2}{({}^{X}AlCl_4^-)^2} \quad (5)$$

From equations (2), (4), and (5), it is possible to derive an equation similar to equation (8) below, from which by a least squares treatment of the Torsi and Mamantov data, the value obtained was $K_2/K_1 = 7.8 \times 10^{-8}$ at 175°C.

The composition region, where K_2 may be evaluated most conveniently, extends approximately from 0.55 mole fraction to 0.70 mole fraction aluminum chloride. The majority of our data were taken in this region. From 10 concentration cells, 63 voltage measurements at different compositions were made. In addition, 8 points were taken with one arm of the cells saturated with NaCl. This common reference point allowed the two different sets of experimental data to be combined. These concentration cell data (excluding the saturated NaCl points) were least-squares-fit to the function

$$\mathcal{E} = a_1(N - N') + a_2(N^2 - N'^2) + a_3(N^3 - N'^3) \quad (6)$$

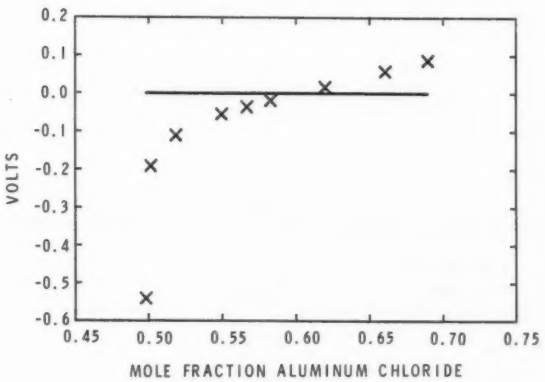

Figure 1. Experimental concentration cell voltages compared with predicted values.
X = voltages obtained in this work;
—— = values predicted from ideal mixing

The complete Nernst equation for concentration cells is

$$\mathcal{E} = \frac{RT}{3\mathcal{F}}\left[4\ln\left(\frac{x_{Cl^-}}{x_{Cl^-_{ref}}}\right) - \ln\left(\frac{x_{AlCl_4^-}}{x_{AlCl_4^-_{ref}}}\right) + 3\ln\left(\frac{x_{Na^+}}{x_{Na^+_{ref}}}\right)\right] \quad (7)$$

The concentrations of the various species required in equation (7) were calculated by an iterative technique from equation (2). The value of K_2 was obtained by curve matching equation (6) with equation (7), the latter obtained by substituting the values of K_0, K_2/K_1, and various trial values of K_2 and K_3 into equation (2). This process led to the value $K_2 = 2.5 \times 10^4$ at 175°C. The only literature report which could provide an alternate calculation of K_2 is the vapor pressure work of Midorakawa et al. (4). At 175°C., their pressure values, which were taken at seven melt compositions between 0.54 and 0.75 mole fraction aluminum chloride, yielded $K_2 = (4 \pm 2) \times 10^4$.

There are no experimental data in the composition region which would be well suited for evaluation of K_3. However, an upper limit of approximately 10^3 may be placed on K_3, because the effect of a K_3 appreciably larger than that would have been noticeable even in the composition region that was explored.

The experimentally determined values of the equilibrium constants are summarized in Table I. The cell voltage data of the present work and that of Torsi and Mamantov (6) are given by empirical equations (8) and (9).

$$\mathcal{E} = -\frac{4RT}{3\mathcal{F}}\ln\left(\frac{1-2N}{1-N} + \left[\left(\frac{1-2N}{1-N}\right)^2 + 4K_2/K_1\right]^{1/2}\right) - 0.7372 \qquad 0.498 \leq N \leq 0.504 \quad (8)$$

Table I
Equilibrium Constants (Mole Fraction Basis) at 175°C

Equilibrium Constants	Values
K_0	2.9×10^7
K_1	3.2×10^{12}
K_2	2.5×10^4 *; $(4 \pm 2) \times 10^4$ **
K_3	$\leq 10^3$ (?)

* From the present concentration cell data.
** From vapor pressures. See Ref. (4).

$$\mathcal{E} = a_0 + a_1 N + a_2 N^2 + a_3 N^3 \quad (9)$$

$$0.51 \leq N \leq 0.71$$

where

$a_0 = -6.9029$

$a_1 = 30.0446$

$a_2 = -44.3122$

$a_3 = 22.3541$

and the reference electrode composition $N' = 0.600$.

Figure 2 illustrates the correspondence between the experimental data and the empirical equation.

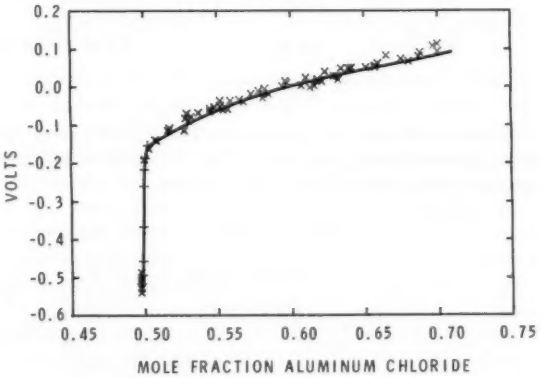

Figure 2. Experimental concentration cell voltages compared with empirical equations.
X = voltages obtained in this work;
+ = values obtained in Ref. (6);
—— = values calculated from empirical equations

Discussion

The extremely large values of K_0, K_1, and K_2 imply a very tightly bound Al^{III}, and therefore enhanced electrochemical oxidation of aluminum anodes. Moreover, the equilibria work to complex the aluminum to a degree markedly dependent upon melt composition. This, in turn, gives rise to the extraordinarily large concentration cell voltages. The composition region in which this behavior has been observed is quite broad; however, to achieve the 0.4 volt increment, the compositions of the two arms of the cell must lie on opposite sides of the 0.5 mole fraction point.

The extent of complex ion formation in molten salt mixtures is cation dependent; that is, the value of the equilibrium constants will vary as the major cation is changed. In aluminum-chloride/alkali-metal-chloride melts, there is evidence (6) that Al^{III} is more tightly bound as one

uses heavier alkali metal cations than Na^+. We intend to explore this observation more fully.

Concentration cell behavior analogous to that observed for the aluminum chloride system should be observable whenever there are a series of very stable complex ions to consume electrode metals. Whether or not any candidate cells would display voltages as high as those observed with aluminum chloride remains to be seen. There is at least one possibility already in the literature; beryllium concentration cells utilizing molten BeF_2-Lif electrolytes have been reported (7) to yield greater than 0.22 volt.

Applications

The use of aluminum anodes in $AlCl_3$-based molten salt electrolytes permits the development of electrochemical power supplies having volume and weight energy densities in excess of anything presently in use, with theoretical energy densitites greater than 700 watt-hours per pound.

A wide melt composition range is available at temperatures ranging from approximately 80°C to several hundred degrees. The low temperature electrolytes should be easy to maintain molten with a minimum of insulation, and may even permit batteries small and light enough to be used in hand-carried equipment.

Other applications include inexpensive thermal batteries of essentially unlimited shelf-life, and warning or alarm devices that are thermally activated at pre-selected temperatures.

REFERENCES

(1) Torsi, G., G. Mamantov, and G.M. Begun, *Inorg. Nucl. Chem. Letters*, 6 (1970), 553.

(2) Vrieland, G.E., and D.R. Stull, *J. Chem. Eng. Data*, 12 (1967), 532.

(3) JANAF Thermochemical Tables, Air Force Contract AF 04(611)-7554, Dow Chemical Company, Midland, Michigan (1965).

(4) Narita, T., T. Ishikawa, and R. Midorikawa, *Denki Kagaku*, 36 (1968), 300.

(5) Smits, A., and J.L. Meijering, *Z. Physikal. Chem. Abt. B.*, 41 (1938), 98.

(6) Torsi, G., and G. Mamantov, *Inorg. Chem.* (in press).

(7) Braunstein, J., K.A. Romberger, and R. Ezell, *J. Phys. Chem.*, 74 (1970), 4383.

X-Ray Photographs of Powder in Vortex Flows

LT B.N. TURMAN
Energy Conversion Research Laboratory, ARL

The study of the behavior of solid particles seeded into a vortex flow has many important applications, ranging from dust filtration to nuclear propulsion (1). In the dust filtration application, dusty gas is forced to rotate inside a confining chamber, and centrifugal force acting on the heavy particles prevents dust from exhausting out the central exit with the gas. Nuclear rocket engine performance may be substantially improved by the adaptation of uranium dust as fuel, which is the basis of the colloid core reactor concept (2). Total surface area of fuel would increase greatly by using small particles (diameters of the order of 1 to 10 microns) as fuel, thereby increasing the heat transfer rate from fuel to propellant and allowing higher power density levels to be maintained in the reactor. The problem of containing the nuclear material within the reactor would be resolved by rotating both the fuel particles and the propellant gas in a vortex flow, applying the principles of the dust separator. Dust separator devices typically operate in the low particle density region, with particle volume occupying some .1% of total volume; the colloid core reactor concept demands a considerably larger particle density, with particle volume on the order of 10% of total volume.

One of the many avenues of research in multicomponent flow being pursued by the Energy Conversion Research Laboratory is the investigation of the particle density distribution in a particle-seeded vortex flow. At large particle density, many techniques useful for measurement in the low density regime become inadequate. Such techniques are light absorption, light scattering, or probe sampling. One method, proven to be well suited for this density regime, is X-ray absorption in which the decrease in intensity of an X-ray beam passing through the vortex flow is related to the density of solid particles present in the flow. The X-ray source used in this experiment is a standard medical unit, operated at peak voltage of 100 KV. Photographic film records the signal intensity at exposure times of about 1 sec. The solid particle for this experiment is talc having a mean diameter of 20 microns.

Figures 1 and 2 are typical X-ray photographs taken of the powder flow

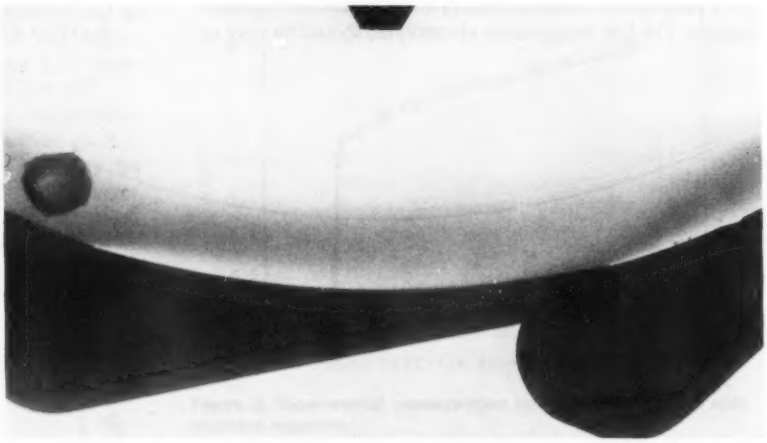

Figure 1. X-ray photograph of vortex flow with 200 gm powder added.

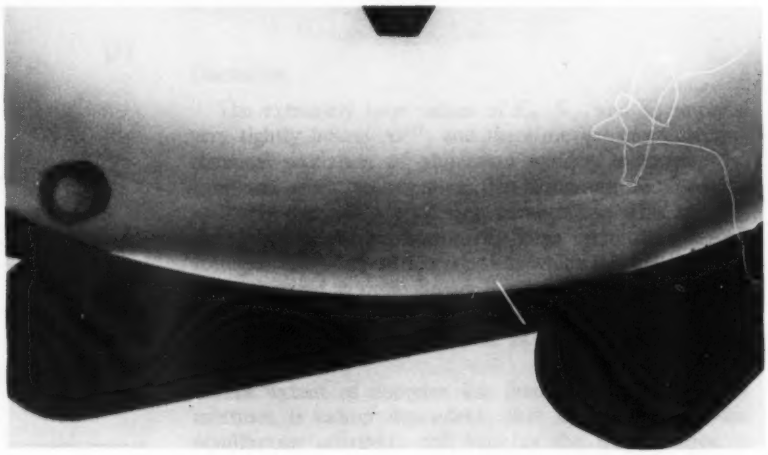

Figure 2. X-ray photograph of vortex flow with 400 gm powder added.

in the vortex chamber. Only a small segment of the complete vortex flow is shown: the peripheral wall of the chamber is made up of an array of 12 of the steel vanes visible in the photographs, with tangential injection of air being accomplished through the overlap region between vanes. Side walls of the chamber are made of plexiglas that is almost transparent to X-rays. Some wall shadows are visible in the photographs, notably the barely visible concentric rings produced by the overlay of two plexiglas sections, the hexagonal shadow of a mounting bolt, and a ragged black circle resulting from a plugged probe-mount hole. The rotating powder flow is clearly visible in these photographs as a medium density shadow above the vane surfaces.

Several qualitative observations can be made from these photographs. The powder is apparently confined within a fairly uniform and well defined ring located at the outer edge of the chamber, with ring thickness increasing as powder is added to the flow. At the vane surface, however, powder density is significantly lower than the average value, apparently because of the interaction between the powder flow and the clear air injected through the vanes. Quantitative analysis of these photographs is possible with the use of a photodensitometer. By measuring the decrease in X-ray intensity, actual powder density in each region of the viewing area can be deduced. Figure 3 shows a density contour map which has been plotted for a total powder load of 400 gm. This contour map illustrates the low density region near the vane and the well defined inner surface of the powder ring. Also appearing on this map are islands of higher density, located just above the injection slot of each vane. Experiment has shown, however, that the size of these islands can be decreased by increasing the energy of the injected gas stream, yielding a more uniform density distribution under appropriate flow conditions.

These observations of particle density within the seeded vortex encourage further studies of the feasibility of the colloid core reactor concept. The density values recorded here represent particle volume fractions near 0.1 (particle volume fraction is the ratio of particle volume to total volume). A calculation of particle volume fraction of nuclear fuel required for criticality in such a reactor has shown that this value would be sufficient to sustain the nuclear reaction (3). The low particle density near the chamber vanes suggests that heat loss to the vane may not be a serious problem. Furthermore, observations of density contours indicate that flow conditions can be adjusted to give uniform density throughout the powder region, providing more efficient mixing of propellant gas with fuel and preventing development of hot spots within the chamber.

REFERENCES

(1) Butt, James D., "Research in Multicomponent Flow," *OAR Research Review*, VII, No. 8 (June 1968), 28-31

(2) Jackomis, W.N., and H.J.P. von Ohain, "Aeromechanical Characteristics of Nuclear Reactor Cavities Using Colloidal Fuels," *AIAA Paper No. 70-1222*, AIAA 7th Annual Meeting, Houston, Texas, October 1970.

(3) Tang, Y.S., J.S. Stefanko, P.W. Dickson, and D.W. Drawbaugh, "An Engineering Study of the Colloid-Fueled Reactor Concept," *J. Spacecraft and Rockets*, 8 (Feb 1971), 129.

Lieutenant Bobby N. Turman has been assigned to the Energy Conversion Research Laboratory, ARL, since 1969. He received the B.S. degree in Physics from the University of Texas in 1965 and Ph.D. in Physics from the same institution in 1968. He is a member of Phi Beta Kappa and the American Physical Society.

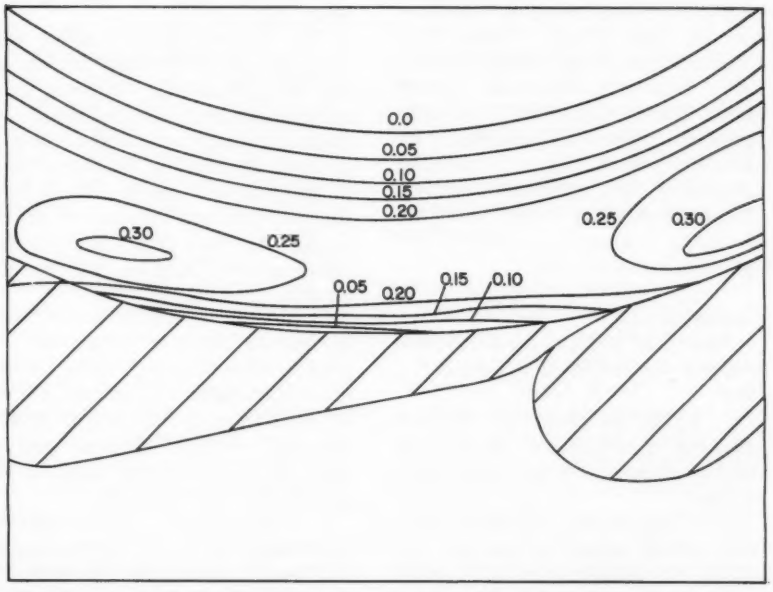

Figure 3. Powder density contours deduced from X-ray photograph plotted for a total powder load of 400 gm.

Inertial Navigation, Guidance, and Control Research

LT COLONEL JOHN PAUL HYDE
Directorate of Aerospace-Mechanics, FJSRL

Introduction

Several months ago, the Frank J. Seiler Research Laboratory, located at the USAF Academy, initiated a new program of applied mathematics research in inertial navigation, guidance, and control (ING&C). The objective of this program is the development and refinement of mathematical models and the description of phenomena, devices, and systems that affect and enable improved navigation, guidance, and control by inertial means. This research is being carried out and documented under FJSRL Project 7904, "Optimization, Programming and Control," the overall objectives of which are to develop mathematical and computational models and techniques for describing, optimizing, or controlling physical systems applicable to designing and evaluating practical aerospace navigation, guidance, control, and communication systems.

Motivation

This new undertaking in ING&C research was motivated by several factors:

a. The Air Force need for fundamental mathematical research on inertial devices, systems, and phenomena.

b. The nucleus of FJSRL scientists already engaged in analytical research on optimization and control theory and techniques, augmented recently by several officers with experience and advanced education in inertial devices and systems.

c. The availability, for active participation and consultation, of the USAF Academy faculty, a large reservoir of exceptional talent in numerous scientific disciplines related and necessary to ING&C research: astronautics and mechanics, geodesy, physics and electronics, and mathematics and computer sciences to assist in modeling, optimization, and data processing.

d. The Academy's Inertial Guidance Laboratory, a high-quality inertial test facility for carrying out experimental verification of theoretical and analytical developments in ING&C research in an academic atmosphere conducive to the conception and exploration of new ideas.

Scope

The ING&C research effort will embrace several different aspects of this field, all aimed at improving inertial guidance and control techniques in future aerospace systems and having a common emphasis on the formulation of mathematical descriptions of inertial principles and instruments as the overall objective. Topics such as the following are being or will be addressed:

a. Gravity Models and Effects on Inertial Systems. Objectives: to develop analytical techniques to improve knowledge and descriptions of the earth's gravity field; and to investigate the effects of different gravitational models and gravity anomalies on inertial system performance.

b. Short-Term Inertial System Performance. Objectives: to investigate and model short-term (10 seconds) precision of inertial sensors and stability-control systems; to study potential improvement needs and approaches; and to recommend system configurations for various known applications.

c. Advanced Analysis and Evaluation Techniques for Inertial Guidance Sensors. Objectives: to investigate error phenomena contributing to inertial sensor inaccuracies and establish pertinent sensitivity coefficients; and to improve the evaluation and analysis methods for determining the sensitivity of inertial devices and systems to environmental parameters.

d. Advanced Gyrocompassing. Objectives: to discern, through mathematical modeling, inertial techniques and requirements which will enable rapid, precise, self-contained azimuth determination. Results will be applicable to both laboratory and anticipated operational needs.

e. Effect of Severe Vehicle Motion on Inertial Navigator Accuracy. Objectives: to determine if certain types of motion excite significant errors; and to select preferable navigator system configurations.

This activity will eventually involve full-time effort by five FJSRL scientists, and several support technicians and engineers; and part-time participation by faculty and cadets of the USAF Academy. When their expertise matches the stated research needs, additional topics will be addressed.

Current Activities

Research is underway in several areas and some results have been published:

a. Knowledge of the earth's gravity field is a major requirement in ING&C systems. The use of ING&C systems in ICBMs and strategic aircraft has increased the importance of an *accurate* knowledge of the gravity field. To date, observations of satellites from ground tracking stations have provided knowledge of the general global characteristics of the gravity field, but have been inadequate for determining localized gravity anomalies because of the relative infrequency of possible satellite observations from

fixed tracking stations.

A new satellite method to obtain direct mapping of the short wavelength anomalies in the earth's gravitational potential has been hypothesized. The method utilizes a pair of satellites, placed in the same nominally-circular orbit, with a small central angle (on the order of 1 degree) between them (see figure 1). The primary data are the onboard measurements of relative velocity between the satellites. As a satellite passes over an anomaly in the gravitational potential, it must change its altitude or its velocity to maintain the proper energy balance. If the anomaly is of a short wavelength, the satellite makes most of the energy correction by modifying its kinetic energy, since a change in velocity occurs more rapidly than a change in position. The only component of satellite velocity perturbation that significantly contributes to such a kinetic energy change is the component that is tangent to the circular orbit. The measurement of relative velocity between the satellite pair is equal to the tangential velocity perturbation of the leading satellite minus the tangential velocity perturbation of the trailing satellite. Hence this relative velocity measures the difference in kinetic energy adjustments required by the individual satellites. This can be converted directly to a measurement of the difference in short wavelength gravitational potential anomalies affecting the two satellites. Proper filtering and summing of the relative velocity measurements provide a direct mapping of the short wavelength components of the gravitational potential encountered along the satellite pair's circular orbit.

Figure 1. Two-satellite method for mapping gravitational anomalies.

b. Improvements in the performance of inertial stabilization systems have generally centered on reducing the long-term drift of an inertial reference frame, an area of particular concern in navigation and guidance systems where substantial flight times are involved (several minutes to several tens of minutes). Known future Air Force applications, however, will require short-term stabilization (on the order of seconds) to an extremely high degree of angular accuracy; e.g., tracking and steering systems, synthetic-aperture radar, and precision release of conventional munitions for close air support (CAS).

An investigation is being undertaken of presently used and new techniques of isolating a stabilized member from angular vibrations induced by a severe dynamic environment. Emphasis is on the postulation and analysis of likely gimbal and motion-sensor arrangements, including the use of angular deviation sensors to detect measurements of base platform motion and to provide proper stabilization commands. Short-term noise characteristics of selected stabilization sensors are being measured experimentally, analyzed, and modeled mathematically so that instrumentation design improvements and/or error-compensation schemes can be recommended. Optimal filtering techniques will be used where applicable to extract actual angular disturbance inputs in the presence of instrument random noise. Models of the mission's dynamic environment will be formulated and described mathematically as required to optimize servo-loop parameters.

c. Improving the accuracy of inertial instruments for ICBM applications requires a better understanding of the instruments' performance over time intervals that are quite short relative to typical boost flight times. Additionally, more knowledge is required of the behavior of an instrument's specific-force-sensitive coefficients at higher acceleration levels.

A new laboratory approach for evaluating inertial gyroscopes has been conceived. This method uses for the first time a precision centrifuge with a counter-rotating platform as a quantitative test bed to provide deterministic specific force inputs to the gyroscope under test. The output data are then analytically fitted to an assumed error model to make the undetermined gyro-error coefficients calculable. In this way an independent solution for all of the classical, specific-force-sensitive drift coefficients is obtained after each five rotations of the centrifuge arm. Previously developed gyro test methods, now in common use, normally require several hours to obtain one solution for the drift coefficients. With the new method, at an input acceleration level of 10 g's on a 260″ radius centrifuge, for example, drift coefficients can be calculated once every 8 seconds. This enables observation and analysis of, and possible compensation for, the short-term variations in individual drift coefficients. In addition, the input-acceleration levels to a gyro that are possible with the centrifuge are appreciably greater than the one-g input provided by existing laboratory tests. Thus, the instrument is exercised in a specific force region that is more representative of its actual operational environment. Laboratory tests are planned to substantiate this theoretical development.

Inertial Guidance Laboratory

Experimental portions of this research program are being conducted in the Academy's Inertial Guidance Laboratory (IGL) which has been dedicated to exclusive support of this program since February 1971. The IGL, designed as a Class 10,000 clean room, is located on the ground floor of Fairchild Hall, an academic building. Within the IGL, a 210-ton steel-reinforced-concrete test pad, with nine integral test piers, floats on 20 pneumatic cylinders that provide isolation in all vibrational modes from external natural and cultural disturbances. The pad and its pneumatic suspension attenuate accelerations from seismic vibrations to a level on the test piers of less than 7 micro-g's at all frequencies from 0.5 to 100 hz under typical

laboratory operating conditions. An active pneumatic stabilization system holds tilting of the test pad about horizontal axes to within 0.1 arc-second per week. Test pad motion is monitored by a seismic monitor station capable of resolutions down to 0.1 micro-g of vibrational acceleration and 0.01 arc second of tilt. Knowledge of these disturbances to such levels of precision, and understanding of their effects on experimental measurements of inertial instruments, enable compensation or correction to further refine and improve the test environment and permit improved interpretation of test data.

Special laboratory equipment includes an automatically-controlled two-axis gyroscope test table, two static accelerometer test stations and associated measurement electronics, an inertial azimuth reference, and various peripheral and data-recording equipment. The test-table allows automatic and repeatable repositioning of inertial sensors to within 0.4 arc second, thereby avoiding uncertainties otherwise introduced into testing through the human element. It also permits continuous long-term experimentation and testing on a 24-hour basis without the need for continual human observation and control.

Summary

A new facet concerning inertial phenomena, devices, and systems for navigation, guidance, and control has been added to FJSRL's program of applied mathematics research. Specific topics within this framework are and will be selected to address critical Air Force needs in this area consistent with the expertise of assigned FJSRL personnel and associated faculty members and cadets. IGL is functioning to support and verify through experiment the theoretical developments of the principal investigators and their associates. The results of this research will enable new or improved concepts and methods for navigation, guidance, and control technology and ultimately will lead to increases in Air Force weapons delivery accuracies.

REFERENCES

(1) Comfort, Capt G.C., "Determination of Gravitational Potential Using Relative Velocity Measurements Between Satellites," *MIT C.S. Draper Lab Report No. T-545*, Cambridge, Massachusetts, June 1971.

(2) Lorenzini, Capt D.A., "A New Gyroscope Centrifuge Test," *Technical Report SRL-TR-70-0018, FJSRL*, December 1970.

(3) Wittry, Lt Col J.P., "Description of an Inertial Test Facility Incorporating a Passively Isolated and Actively Stabilized Platform," *Paper No. 69-863*, presented at the *AIAA Guidance, Control, and Flight Mechanics Conference*, Princeton, N.J., 18 August 1969.

Capt Dino A. Lorenzini, FJSRL Research Associate, and Capt Harvey T. Brock, USAFA Assistant Professor of Astronautics, examining the details of a gyro test table in the Inertial Guidance Laboratory

Capt Dino A. Lorenzini, FJSRL Research Associate, and Capt Harvey T. Brock, USAFA Assistant Professor of Astronautics, examining the details of a gyro test table in the Inertial Guidance Laboratory.

Approximation Theory

DR. O. SHISHA
Applied Mathematics Research Laboratory, ARL

Introduction

Approximation theory is a branch of mathematics devoted to the approximation of general functions, curves, and surfaces by "simple" ones. Much of the theory is concerned with the approximation of arbitrary real functions f, continuous in a finite interval $a \leqslant x \leqslant b$, by polynomials.

The need for such approximation is clear: a given function may be too complicated to be handled; therefore, we would like to substitute a simpler, more manageable one, even though the new function differs slightly from the original.

Some of the questions that arise immediately are: What kind of "simple" functions, curves, and surfaces should be considered for approximations? How does one measure the "goodness" of a given approximation? Is there always a "good" approximation and, if so, how "good" is it?

Although approximation theory is an old field, it has undergone an unusual revival in the last 20 years due to the development of high speed electronic computers. Workers in the field are now concerned, not merely with the above and other theoretical questions, but also with the numerical computation of approximations, using computers.

Some Applications of Approximation Theory

By the very nature of approximation theory, it is not surprising that its methods and techniques are of vital importance in many fields of the physical sciences and engineering, including domains of great significance to the Air Force. Some examples are quite old. For instance, to find areas of regions bounded by curves, one considers the curves to be approximately graphs of third degree polynomials to which Simpson's rule can be applied. In the design and construction of curved portions of highways and railroads, these portions are approximated by circular arcs, parabolas, cubic parabolas, and various spirals. A more recent example is the approximate representation of automobile body surfaces by simpler surfaces, in a manner readily handled by electronic computers. Professor G. Birkhoff of Harvard University, in collaboration with the mathematics staff at the General Motors Research Laboratories, has studied quite successfully (using spline functions) this problem which is of great interest to the automobile industry. No doubt exists that similar results can be obtained for air and space craft.

In general, whenever one has to apply mathematical theories to functions, curves, or surfaces that are too complicated to handle, one looks to the methods of approximation theory to devise simpler replacements. In particular, approximation theory plays an important role in the solution of engineering problems leading to ordinary or partial differential equations, or involving linear or nonlinear programing, optimal control, and other mathematical theories.

Approximation Theory at ARL

Aerospace Research Laboratories has been an important center for approximation theory because of the work done at ARL and the fact that the Editor of the Journal of Approximation Theory is a member of the Laboratories.

An article (1) by the author introduced a new subject in approximation theory; namely, monotone approximation, which has inspired much further study by some of the chief workers in approximation theory.

As stated in the Introduction, a typical situation in problems of approximation theory is that of a real, continuous function f(x) to be approximated over an interval $a \leqslant x \leqslant b$ by polynomials, i.e., functions of the form

$$p(x) = a_0 + a_1 x + a_2 x^2 + \cdots + a_n x^n$$

in which the a's are constants.

We can often think of such a polynomial, associated with f(x), as being generated by some "operator" operating on f(x). A natural and most important question is: Given a function f(x) and such an operator, how close is f(x) to p(x)?

For the important case in which the operator under consideration is linear and positive, a general answer (2) was given by the author and B. Mond. They gave a formula which estimates the closeness of f(x) to p(x) for an arbitrary continuous function f(x), provided one can make this estimate for the three simple functions $f(x) = 1$, $f(x) = x$, $f(x) = x^2$ (or for three other simple functions). Since handling such simple functions is usually very easy, a straightforward procedure is available for estimating the closeness of f(x) to p(x) for arbitrary continuous functions f(x). This work gives a quantitative, computable form to a previous theoretical result of P.P. Korovkin.

Article (2) appeared in August 1968, followed by a

second article (3) by the same authors on the same subject. Other mathematicians, both in the U.S. and abroad, at once followed with similar work. Though just recently published, these results are already considered as standard and fundamental in approximation theory.

The author is the Editor of the Journal of Approximation Theory, the only periodical devoted exclusively to approximation theory. On its editorial board, besides the Editor, are 19 Associate Editors. This group consists of the finest workers in the field in the U.S., as well as several outstanding European mathematicians. They include: Professor G. Birkhoff of Harvard University; Professor S. Karlin of the Weizmann Institute of Science and Stanford University; Professor G.G. Lorentz of the University of Texas; Professor I.J. Schoenberg of the Mathematics Research Center, University of Wisconsin; Professor J. Todd of the California Institute of Technology; and Professor J.L. Walsh, a Harvard University retiree, presently at the University of Maryland.

The editorial work for the Journal of Approximation Theory helps ARL maintain leadership in the field. By receiving all Journal manuscripts long before their publication, and through correspondence with the authors about their manuscripts, ARL keeps informed of the current state of the art. The wide acquaintanceship of the Editor with past, present, and potential contributors to the Journal enables him to obtain the finest data available on problems in which he or his colleagues are interested. For example, ARL has recently received, at the Editor's request, the finest computer programs available on approximations by polynomials, rational functions and spline functions. Hopefully, this material will prove beneficial in solving future Air Force problems.

Conclusion

ARL expects to continue as an important center for approximation theory. Under study are linear positive operators, spline functions, and some geometrical extremal problems; further work is planned. New computing equipment now being installed will extend the applicability of approximation theory to concrete problems of the Air Force. The expected rapid development of approximation theory in the 70's should play a significant role in advancing future Air Force technology.

REFERENCES

(1) Shisha, O., "Monotone Approximation," *Pacific Journal of Mathematics*, Vol. 15 (1965), 667-671.

(2) Shisha, O. and B. Mond, "The Degree of Convergence of Sequences of Linear Positive Operators," *Proceedings of the National Academy of Sciences*, Vol. 60 (1968), 1196-1200.

(3) Shisha, O. and B. Mond, "The Degree of Approximation to Periodic Functions by Linear Positive Operators," *Journal of Approximation Theory*, Vol. 1 (1968), 335-339.

Dr. Oved Shisha has been with the Applied Mathematics Research Laboratory, ARL, since 1962. He is working on approximation theory and other areas of mathematical analysis.

Dr. Shisha received both his M.S. (1955) and his Ph.D. (1958) in Mathematics from the Hebrew University, Jerusalem, Israel. From 1958 to 1960, he was a research fellow at Harvard University and from 1960 to 1962 he was employed as a mathematician at the National Bureau of Standards, Washington, D.C.

In 1965, Dr. Shisha edited the proceedings of a "Symposium on Inequalities," sponsored by ARL and made up of 24 papers contributed by some of the greatest living mathematicians. In 1967, he edited the proceedings of a "Second Symposium on Inequalities" sponsored by ARL and FJSRL. Dr. Shisha is co-editor of a book, entitled "Studies in Approximation and Analysis," with Professor J.L. Walsh of Harvard University.

Dr. Shisha is a member of the Mathematical Sciences Section of the Ohio Academy of Science, the Dayton Section of the Society for Industrial and Applied Mathematics, and Sigma Xi.

Scientific Notes

OXIDATION OF TITANIUM-ALUMINUM-GALLIUM ALLOYS

Metals and Ceramics Division, AFML

In-house research at AFML has resulted in a marked improvement in the oxidation resistance of titanium-aluminum alloys with gallium additions. Continuous weight-gain measurements at temperatures in excess of 600°C showed that, with increasing equimolar proportions of Al + Ga, the overall oxidation decreased. Parabolic behavior is normally observed, even at 950°C, although at this higher temperature interruptions (rate increases) are common. This improvement may be directly related to gallium rejection from the growing scale and subsequent reduction in the oxygen diffusion rate. These results indicated a much lower diffusion rate (an instantaneous rate, decreasing with time) than that observed for the pure metal.

Results of this research were presented at the recent TMS-ASM Joint Meeting in Cleveland, Ohio, in the Environmental Reactions I session. The paper, "Oxidation Behavior of Titanium-Aluminum-Gallium Alloys," was prepared by Dr. S. R. Lyon and Dr. H. L. Gegel of the Advanced Metallurgical Studies Branch, Metals and Ceramics Division, AFML, and J. Schell of the University of Cincinnati.

The effect of aluminum on the oxidation behavior of titanium has been studied by a number of workers, but results are somewhat contradictory. The trend from such work indicates little direct benefit from aluminum.

Although no work has been reported on the effects of gallium on oxidation properties of titanium-based alloys, this knowledge is essential in the contemplation of gallium additives for high-temperature, high-strength alloys.

Current titanium alloy development for useful 900°F + alloys generally attempts to evaluate that proportion of property degradation caused by air contamination (i.e., not due to metallurgical instability). It has been shown that a causal relationship exists between air contamination rate and rate of property degradation (ΔRA%). In studies of the rate of air contamination (depth of oxygen diffusion in the alloy to a certain oxygen level) versus temperature, for all titanium alloys studied to date, contamination was observed to be faster than in the pure metal, but among the alloys there was only a difference factor of 2. The effect of gallium is thus far unique in that a reduction of oxygen penetration occurs. This study is continuing with long term exposures at lower temperatures in air to quantitatively relate the reduction of oxygen diffusion to gallium rejection at the alloy-oxide interface.

Contact: Dr. C. T. Lynch, AFML/LL
Telephone Ext. 55309

FRACTURE MECHANICS OF FIBER REINFORCED LAMINATED PLASTIC COMPOSITES

Non-metallic Materials Division, AFML

The field of fracture mechanics is a major discipline needed in the analysis of composite structural elements for aerospace vehicles. In particular, a theory of crack propagation within the layers of a fiber reinforced laminated plastic composite is needed to define material properties that measure crack propagation resistance. With such a theory, fracture experiments can be properly interpreted and analysis of structures with pre-existing flaws can proceed on a rational basis.

The basis for such a fracture theory has been developed by Drs. G. C. Sih and R. P. Wei, of Lehigh University, under contract to the Plastics and Composites Branch, Nonmetallic Materials Division of AFML.

The analysis of the stresses in the region of a crack tip in the resin phase of a unidirectional composite was determined, and equations were developed to predict the onset of unstable crack propagation. Experiments have also shown a significant influence of fiber volume fraction on the resistance of a composite to crack propagation. In fact, an apparent optimum volume fraction has been observed that may have significant consequences in the application of composite structures. More work is being conducted to substantiate this finding.

Before the study of the fracture of anisotropic laminates, several pilot problems in which the layers are isotropic were studied. An important result of this study has been the definition of stable/unstable regions of crack propagation in such a system; that is, under certain conditions the stresses in front of an advancing crack are reduced and the process can be self-arresting.

Additional analytical and experimental work is now being conducted, using this work as a basis to treat the more general problem of the fracture mechanics of laminated composites (as opposed to unidirectional composites) containing anisotropic layers.

Contact: Dr. N. J. Pagano, AFML/LN
Telephone Ext. 52389

MASS SPECTROMETRIC DETERMINATION OF VOLATILE ELECTRODE PRODUCTS

An important method has been found to permit analysis of the gaseous products of electrochemical reactions as they occur. This advance allows the products of electrode-electrolyte reactions to be sampled directly during the reaction. A major difficulty in elucidating the fundamental processes of these reactions, such as occur in batteries and fuel cells, is the chemical reactions that occur between electrode products and other species present in the solution before an analysis can be made.

The new method uses a special porous electrode, one side of which contacts the solution being electrolyzed, with the other side in contact with a mass spectrometer's high-vacuum system. This technique is proving extremely valuable in the study of electro-chemistry of organic materials proposed for use in fuel cells. The SUNY Buffalo development is reported in the *Journal of the American Chemical Society*, 93 (1971), 793.

SUPERSONIC TURNS WITHOUT SUPERBOOMS

Some of the most destructive sonic booms are those focused by the curvature of the bow wave on the inside of a turn. Studies of this phenomenon were carried out for AFOSR by the University of Toronto Institute for Aerospace Studies. The Institute has suggested that this focusing effect can be suppressed by moderately slowing the aircraft during the supersonic turn. Steady speed supersonic flight produces a straight line (conic) shock wave. A steady speed turn creates a curved front that converges the sound rays into a limited area on the ground. But a slowing turn forms a straight line shock front with no subsequent superboom, and the rate of slowing has been shown to depend upon the rate of turn. An optimum solution could be provided by an onboard computer linked to the controls. This work was presented at the annual meeting of the American Institute of Physics, Washington, D.C., 20-23 April.

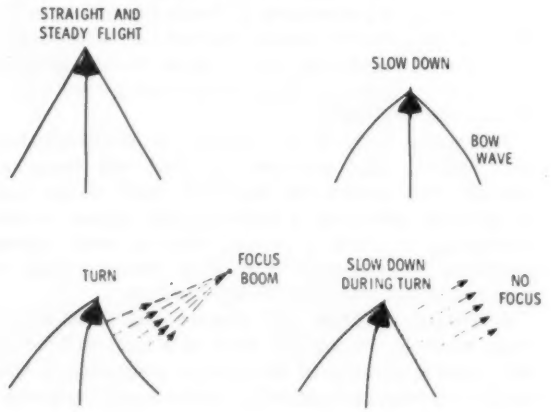

BOW WAVE OF SUPERSONIC AIRCRAFT IS CONCAVE ON INSIDE OF TURN, LEADS TO FOCUS BOOM. SLOW-DOWN CURVES WAVE OPPOSITELY. COMBINED SLOW-DOWN AND TURN YIELDS STRAIGHT BOW WAVE, NO FOCUS.

STUDIES TO IMPROVE RADAR TARGET PERCEPTION

A major problem in radar operation is distinguishing targets from noise and clutter. Methods to assist this task include displays that accentuate the coherent motion of targets relative to random noise and moving clutter.

One well-known technique is the storage of successive radar images for playback at a faster rate, causing the target to appear as a rapidly moving dot. Detection has been shown to be further enhanced by various combinations of numbers of prior-image frames and different time compression ratios, or by using simultaneous presentation of stored frames.

Under AFOSR contract, the University of Illinois is undertaking (1) to determine and measure for the first time the effects of time compression variables upon detection performance, and the interactions of these variables, and (2) to relate existing time compression data to the human perceptual process.

During the past year, the radar and task simulation has utilized a target and noise generator, a flying spot scanner, a digital scan converter with disc storage, and a cathode ray tube display. This equipment is to be supplemented with the Navy TICODS system (Naval Electronics Laboratory).

As with all complex perceptual phenomena, the central problem is the identification and analysis of the attributes of the stimulus that effectively govern the response. In radar visual time compression phenomena, the number of relevant stimulus variables is quite large, and their combinations are beyond calculation. The results of first experiments indicate a potential two-to-one decrease in the detection time of targets in noise and clutter by using various techniques to match the display to the human perceptual system.

Contact: Dan Taylor/AFOSR
Telephone Ext. 44875

LOW TEMPERATURE INFRARED SPECTROSCOPY OF HYDROGEN BONDED POLYMERS

Materials Physics Division, AFML

It has been known for about 20 years that when the infrared spectrum of a low molecular weight solid hydroxy compound is recorded at liquid nitrogen temperature, the spectrum obtained is often a great improvement over that obtained at room temperature. However, a number of authors have alleged that this improvement is only a property of low molecular weight, crystalline compounds and would not be of use to characterize the commercially important higher molecular weight materials of these chemical classes. An investigation recently completed in the Analytical Branch, Materials Physics Division, indicated that these assumptions are incorrect and that, if proper precautions are taken in sample preparation, substantial gains in information can be realized by low temperature infrared spectroscopy.

The key to success involves selection of extremely crystalline samples for study. Such samples can be obtained in two ways. First, model systems can be selected which are naturally occurring, highly crystalline analogs of commercial polymers. Second, commercial materials can be increased in crystallinity by selective extraction of the less crystalline areas. The development of such techniques should allow considerable new insight into the solid state properties of many important hydrogen bonded materials such as cotton, rayon, and the various nylons and other fabrics of Air Force interest.

Contact: Captain H. A. Wells, AFML/LP
Telephone Ext. 55036

EROSION MECHANISMS OF GRAPHITE MATERIALS

Materials Support Division, AFML

The initial part of a program to investigate erosion mechanisms and improvement of graphitic materials has been completed by the McDonnell Douglas Western Division under contract to the Space and Missile Systems Support Branch, Materials Support Division, AFML. The purpose of this program is to study in detail the composition and physical variables of graphitic material which influence the erosion mechanisms and contribute thermochemically and thermomechanically to the ablation process.

Nine different graphite materials, which were fabricated in-house or chosen from those made available by commercial producers, were studied to provide representation of the spectrum of variables of principal materials. These materials contained variations in filler type and size from the large platelet pyrolytic particle to the small equiaxial Santa Maria particle, with further variations in binders such as glassy carbon versus the thermoplastic and impregnant type. Further variations included consideration within a specific formulation of microstructure as influenced by processing, i.e., variable percentage porosity.

These materials were subjected to characterization such as surface roughness (optical and stylus), density (bulk, submerged, and helium), pore size distribution (optical, mercury, and nitrogen adsorption), microstructure, permeability, hardness, and crystallographic X-ray determination. They were then exposed to sublimation tests for 20 minutes at 3000°C and separately to oxidation tests for 1 minute in flowing air at 3000°C. After test, they were recharacterized to determine structural and compositional changes, with first correlations showing that an in-depth change occurs that is strongly dependent on the total surface area characteristics of a material and is relatable to the mass loss. Other noted changes occur in preferential removal of the binder and etching of pores.

A complete analysis of the data and information gathered to date is being incorporated into the Phase I report by McDonnell Douglas. Because of the high interest in this activity, periodic meetings have been held to convey information to aerospace industry contractors, NASA, AEC, Aerospace Corporation, and SAMSO.

The program at McDonnell Douglas is continuing with high pressure arc testing of the materials to determine the importance of laboratory findings under simulated flight environmental conditions.

Contact: Mr. C. A. Pratt, Jr., AFML/LA
Telephone Ext. 53691

COMPRESSIVE BEHAVIOR OF UNIDIRECTIONAL FIBER REINFORCED PLASTIC COMPOSITES

Nonmetallic Materials Division, AFML

The scientific treatment of the problem of composite material design (i.e., the determination of constituent material properties, size, and relative proportions for optimum performance under compressive loading conditions) is hampered by the absence of a theory of compressive failure. One particular concern is the determination of a condition for compressive failure to occur by the mechanism of microbuckling, where fiber instability triggers the fracture process.

Preliminary compressive experiments on model systems have been performed by L. B. Greszczuk of McDonnell-Douglas under contract to the Plastics and Composites Branch, Nonmetallic Materials Division, AFML, in an attempt to isolate the significant parameters governing microbuckling. Greszczuk's experiments demonstrate rather conclusively that microbuckling can occur. The qualitative relationship between this behavior and fiber and resin properties and geometric parameters (specimen length, width, and volume fraction) were demonstrated. Initial experiments were performed under conditions involving, for example, very soft resin material and high aspect ratio which encourage microbuckling failures. Failures in these tests occurred at composite stresses that were much lower than those resulting from true fiber compression failures of overall instability. At the other extreme, for conditions which are probably more representative of structural composites, other failure modes with attendant higher stress levels were observed, such as fiber compression and resin cracking.

Current work under this program involves a more extensive study of the manner in which phase (fiber and resin) properties and geometry influence the various failure modes. Analytical, as well as experimental work on model systems is being conducted. In addition, the conclusions will of course be checked against experimental results on actual fiber reinforced plastic composite samples. Laminated composites will be considered as well as unidirectional, but the latter, being basic to understanding the phenomena, are being investigated first.

Contact: Dr. N. J. Pagano, AFML/LN
Telephone Ext. 52389

NEW, IMPROVED SHIFT REAGENTS FOR SIMPLIFYING NMR SPECTRA

Materials Physics Division, AFML

A collaborative study between Roger E. Rondeau of the Exploratory Studies Branch, Materials Physics Division, and Dr. Robert E. Sievers of the Aerospace Research Laboratory, has resulted in the development of materials that are proving a boon to Nuclear Magnetic Resonance (NMR) spectroscopists. The materials are europium and praseodymium chelates which, when added to NMR samples, dramatically simplify their spectra by inducing spectral shifts. These shift reagents are vastly superior to any previously reported in the literature. They can be used to simplify complex spectra, elucidate structure, and facilitate spin decoupling experiments. Previously uninterpretable spectra become easily resolved through the use of a few milligrams of the improved shift reagents. The europium chelate causes downfield shifts, while the praseodymium chelate shifts the spectral peaks in the opposite direction. Used in combination, these materials are powerful tools for NMR spectral interpretation and structure elucidation. Both chelates have been used by Mr. Rondeau to determine the structure of a large number of liquid crystals. In fact, where conventional chromatographic techniques have failed to separate isomeric mixtures of liquid crystals, the application of the shift reagents has afforded the spectral separation of the isomers.

Thus, through a cooperative effort between AFML and ARL, improved shift reagents have been developed that greatly simplify spectra and make them much easier to interpret. This is expected to have a great impact on the entire field of materials characterization and analysis. The reagents should be useful in the NMR characterization of any number of materials of special interest to the Air Force, including adhesives, seals, glues, coatings, colorants, oils, lubricants, solvents, fluids, propellants, fuels, and intermediates in the synthesis of these products. Frequently, complex spectra can only be simplified by obtaining higher frequency spectra—an often necessary but extremely costly expedient. The use of these newly developed reagents to accomplish the same or even better spectral simplification can be an economical substitute. To convert NMR spectrometers, presently widely available in chemical laboratories, to very high frequency instruments can cost in excess of $100,000, while some of the same advantages can be realized chemically rather than instrumentally by the judicious selection and use of NMR shift reagents.

Mr. Rondeau introduced these new materials in an invited lecture at the 12th Experimental NMR Conference in Gainesville, Florida, 18 February 1971. The two chemists have also co-authored a paper soon to appear in the Journal of the American Chemical Society.

The civilian and commercial interest in these materials has been enormous. One chemical company has named the shift reagents after Mr. Rondeau and Dr. Sievers, and estimates at least 1000 buyers per year.

Contact: Dr. H. M. Rosenberg, AFML/LP
Telephone Ext. 52280

YTTRIUM ORTHOALUMINATE – IMPORTANT NEW LASER HOST MATERIAL

Materials Physics Division, AFML

Large single crystals of yttrium orthoaluminate ($YA10_3$) were grown for the first time in 1967 and 1968. The crystal growth method used was a hollow cathode float zone process being developed under AFML sponsorship (reported in AFML-TR-67-57 and AFML-TR-69-4). This work showed that $YA10_3$, previously thought to be an unstable incongruently melting compound, in fact crystallizes easily and furthermore can accept large amounts of rare earth dopants. It was concluded, therefore, that $YA10_3$ could be easily grown by Czochralski pulling from iridium crucibles and that the melt-crystal distribution coefficient for a rare earth such as neodymium would be close to unity.

Early in 1969 the Raytheon Company verified the conclusions drawn from the hollow cathode work by pulling large, laser quality crystals of $YA10_3Nd^{3+}$ directly from the melt. The distribution coefficient for Nd^{3+} was, in fact, found to be close to unity. This large distribution coefficient makes it possible to pull neodymium doped crystals at much faster rates than are possible with yttrium aluminum garnet (YAG) in which the Nd^{3+} distribution coefficient is only 0.18. Since much faster pull rates mean much lower laser rod costs, the new host could potentially replace YAG as the most popular laser material.

It remained to verify that $YA10_3$ lasers could perform as effectively as YAG lasers. To do this, the Raytheon Company was awarded a contract with the AFML to perform laser studies on $YA10_3$. Results of the Raytheon Company study are reported in AFML-TR-70-258. A brief summary of the results are given here. Laser action in $YA10_3:Nd^{3+}$, $YA10_3:ND^{3+} + Cr^{3+}$, and $YA10_3:HO^{3+} + Ey^{3+} + Tm^{3+}$ was observed. For all systems studied, $YA10_3$ exhibits low gain and high gain orientations. A $YA10_3:Nd^{3+} + Cr^{3+}$ rod oriented along a low gain direction was shown to have a saturable output in Q-switched pulse operation of more than twice that of the best $YAG:Nd^{3+}$ rod available. It was also concluded that in the high gain orientation, $YA10_3:Nd^{3+}$ or $YA10_3:Nd^{3+} + CR^{3+}$ should perform better than YAG in CW operation because of the natural bi-refringence of $YA10_3$. Further work along these lines will be carried out in a follow-on effort at Raytheon.

In the meantime, commercial suppliers have begun to sell $YA10_3$ laser rods. Recently quoted prices for $YA10_3:Nd^{3+}$ rods range from 60 to 80 percent of the prices for $YAG:Nd^{3+}$ rods, with the lower percent figure applying to the largest rods. The achievement of these lower prices less than 18 months after the first laser tests on $YA10_3$, together with the encouraging laser test results at Raytheon, are strong indications that this material will live up to the original expectations and will become the leading laser host material.

Contact: Vincent L. Donlan, AFML/LP
Telephone Ext. 52280/52110

READER
INTERCHANGE

Invention Disclosures

Contact: Colonel Ludwig Lippert, AFOSR/JA
Telephone Ext. 45054

DDC for documentation on the Air Force contract

Epoxy Resistance Thermometer

A thin layer of an epoxy silver filled conductive adhesive, which displays an essentially linear resistance-temperature characteristic in the temperature ranges from 4.2°K to 373.16°K (100°C), has been developed. (Developed by Stuart Kasdan, Radio Corporation of America, AF Contract AF49(638)-1223.)

ID-71-18

Method of Fabricating Lightweight Targets for Radar Measurements

A method has been proposed of fabricating radar target models, a method especially applicable to bodies of revolution, that is, axi-symmetric bodies. The proposed finished model is dimensionally accurate, rugged, and extremely light. (Developed by S. Abrams, J. De Luca, I. Weissman, and K. Weil, Columbia University, AF Contract AF49(638)-1113.)

ID-71-19

Transfer Discharge Ion Getter Vacuum Pump

The pump consists of two co-axial cylindrical anodes between the titanium cathode plates. In addition to a high positive potential of 3 to 5 kilovolts, now connected to both anodes, a few hundred volts of high frequency alternating potential are applied between the cylindrical anodes. (Developed by K. R. MacKinzie, University of California, AF Grant AF-AFOSR 567-64).

ID-71-20

Deflection Modulation Display

Deflection Modulation Display is a technique of presenting three-dimensional data visually, a technique similar to television and oscilloscope display. A novel method of controlling the cathode ray tube electron beam yields a depiction of third dimensional data on a conventional screen. (Developed by T. E. Everhart, University of California, AF Grant AF-AFOSR-139-64.)

ID-71-21

Boundary Layer Probe

A probe, denoted as pressure probe, is used to measure impact pressure profiles when air is used as the secondary gas. The probe senses the dynamic head in the boundary layer at the location of its tip when attached to a freestream static-pressure probe. (Developed by C. J. Scott, University of Minnesota, AF Grant AF-AFOSR-17-64.

ID-71-22

Improved NMR Probe for Magnetic Field Measurements

A small, simple, transistorized, marginal-oscillator type nuclear magnetic spectrometer has been developed for high resolution mapping of magnetic fields in relatively inaccessible locations, such as the interior of superconducting solenoids. With a probe volume of 8×10^{-6} liter, the device is able to give magnetic flux-density measurements having an accuracy of 2 parts in 10^6 with a spatial resolution of about 1 mm. Remote operation of all controls adds considerably to its versatility. (Developed by W.L. Pierce and J.C. Hicks, Oregon State University, AF Grant AF-AFOSR 510-64.)

ID-71-23

A Wideband, Low Noise Frequency Modulator That Can Be Used for Rapid Modulating Rates

A varactor diode with a Clapp oscillator circuit to greatly increase deviation bandwidth while maintaining low noise and high operational speed has been used. (Developed by Leon Baum, Columbia University, AF Contract AF49(638)-1113.)

ID-71-24

Research Advances

Exoatmospheric Infrared Calibration

Nature of Result: The variation in surface temperature of Mars, as a function of latitude and season, has been computed.

Significance: The surface temperature of Mars, and hence the total radiance from the planet, changes drastically with changing insolation because Mars lacks the "greenhouse" protection of a thick atmosphere. Because Mars, like the earth, has an axis of rotation that is tilted at more than 20 degrees to its orbital plane, seasonal effects on insolation are large. In addition, the ellipticity of its orbit causes a 43 percent annual change in total insolation. The combination of seasonal and orbital changes in insolation results in complex latitude-dependent surface temperature variations that affect the total radiance of the planet as seen from the earth. These surface temperature variations have been computed in detail, and can be integrated to yield the total radiance of the planet as seen from the earth as a function of time.

RA AFCRL 70-17

Contact: Dr. John W. Salisbury, AFCRL/PHL
Telephone Ext. 4622

Langmuir Probe Data Reduction Program

Nature of Result: A computer program has been developed to reduce characteristic Langmuir probe curves and provide the user with information on the following plasma parameters: electron temperature, number density, and energy distribution function. The program is based on collisionless probe theory in the calculation of the plasma parameters.

Possible Applications: This program can be used to process probe data which are being recorded on magnetic or paper tape. The basic inputs are initial and final voltage and the recorded current readings from the characteristic curves. The program may be easily adapted for use by any facility that uses Langmuir probes to provide plasma diagnostics. The program, written in Fortran IV, can be modified to handle the user's particular input.

RA ARL 71-1

Contact: Captain William F. Bailey, ARL/ARH
Telephone Ext. 3835

Effect of Unsymmetrical Nose-Bluntness on Stability Derivatives

Nature of Result: In the analysis of the free flight motion of bodies of revolution, the tricyclic theory assumes that a small configurational asymmetry does not violate the rotational symmetry of the stability derivatives in pitch and yaw, but does produce a non-zero trim angle. However, tests made by scientists at Mach 14 in ARL's 20-inch Hypersonic Wind Tunnel show that a small unsymmetric nose-bluntness destroys the rotational symmetry of the stability derivatives of a slender cone at hypersonic Mach numbers. These test results invalidate the basic assumption of the tricyclic theory.

RA ARL 71-2

Contact: Mr. O. Walchner, ARL/ARR
Telephone Ext. 54596

Passive Optical Techniques for Space Object and Target Identification

Nature of Result: ARL has demonstrated non-imaging optical techniques for the identification or assessment of space objects. These techniques use a relatively small tracking telescope to make low cost measurements in a way characteristically different from radar techniques. Some characteristics and capabilities are:

(1) Utilizes the sun's continuous illumination of the target - no PRF limit.
(2) Inherently bi-static, allowing immediate ambiguity resolution.
(3) Distinguishes easily between different surface coatings and small surface features.
(4) In many instances, permits precise determination of shape and dynamical motion.
(5) Allows separation of associated targets that are only a few tens of meters apart.
(6) Provides positive checks on radar space object identification (SOI).
(7) Obtains SOI data at much greater ranges than radar can.

Possible Applications: Some specific applications include precise measurements of stability and dynamics of spin-table payloads and the immediate identification of components of new launches where the component radar signatures may be similar or where components separate slowly.

References:

Kissell, Kenneth E., "Advantages of a 4-axis Tracking Mount for the Photoelectric Photometry of Space Vehicles," *ARL 65-260*, December 1965.

Vanderburgh, Richard C., "A Prediction and Tracking Method for Small-Aperture, Continuous Optical Tracking of Artificial Satellites," *ARL 66-0008*, January 1966.

Kissell, Kenneth E., "Diagnosis of Spacecraft Surface Properties and Dynamical Motions by Optical Photometry," *ARL 69-0082*, May 1969, Reprinted from Space Research IX - North Holland Publishing Company, Amsterdam (1969).

Kissell, Kenneth E., "Proceedings of the University of Miami Symposium on Optical Properties of Orbiting Satellites," *ARL 69-0078*, May 1969, (Contract F33615 67 C 1870).

Vanderburgh, Richard C., and Frank R. Vigneron, "Passive Optical Measurements of Alouette II Spin Dynamics," paper presented at COSPAR Symposium, Prague, May 1969.

Vanderburgh, Richard C., "Results of Field Testing an Inexpensive Transportable Photoelectric Satellite Tracking System," paper presented at COSPAR Symposium, Prague, May 1969.

Vanderburgh, Richard C., "Wide Band (Visual Spectrum) Photoelectric Photometry of PAGEOS During its First Fifteen Months in Orbit."

Vanderburgh, Richard C., and Kenneth E. Kissell, "Measurement of Deformation and Spin Dynamics of the PAGEOS Balloon-Satellite Photoelectric Photometry."

Kissell, K. E., and R. C. Vanderburgh, "Initial Results of Simultaneous Radar-Optical Signature Measurements," Proceedings of the GISAT II Symposium Vol. II, Part II, (163-200) AD 392,700 (SECRET).

Kissell, K. E., and R. C. Vanderburgh, "Photoelectric Photometry–A Potential Source for Satellite Signatures," Proceedings of the 1st GISAT Symposium (1965) AD480-500 (CONFIDENTIAL).

Kissell, Kenneth E., "Optical SOI ARL Photometry Developments," Proceedings of the Second NORAD Space Identification Conference (U), pp. 25-46 (SECRET).

"Required Operational Capability (ROC) for Electro-Optical Sensors for Space Surveillance (U)," ROC: ADC 1-71, 31 Mar 71 (SECRET).

Kissell, Kenneth E., "Report of NORSIC 2 Working Group 5: Optical SOI," Proceedings of the Second NORAD Space Identification Conference (U), pp. 169-183 (SECRET).

RA ARL 01-71-3

Contact: Mr. Kenneth E. Kissell, ARL/LG
Telephone Ext. 54833

New Centrifuge Test Method for Inertial Gyroscopes

Nature of Result: A new centrifuge test method for the extraction of gyro performance model coefficients over very short time intervals has been developed and analyzed.

Significance: This test method will substantially reduce the time necessary for a complete performance model solution. In this way, short-term variations of inertial gyroscopes can be observed and analyzed.

Possible Applications: This test can be implemented on a large, precision centrifuge with a counter-rotating platform to evaluate gyros intended for bal issile applications.

RA FJSRL 70-8

Contact: Captain Dino A. Lorenzini, FJSRL/NA
Telephone Ext. 3121

Model for a Short-Range Dogfight Missile

Nature of Result: A simple mathematical model for a short-range dogfight missile has been developed along with a method for determining certain specifications for a missile to satisfy given performance requirements.

Significance: The model enables the finding of acceptable approximate weight, diameter, wing area, propellant mass, thrust level, and other quantities for a short-range dogfight missile.

Possible Applications: Method could serve as a rough check of contractor studies. An experienced missile designer should be able to produce a design that meets all the criteria, and has as small a launch weight as this method predicts. These results are based on well known and obtainable aerodynamic and solid-rocket-engine performance characteristics. The model can be used in reviewing missile designs proposed by aerospace contractors, or in developing new specifications for advanced versions.

RA FJSRL 70-2

Contact: Captain Roger W. Gallington, FJSRL/SLA
Telephone Ext. 3122

The Ram-Wing: Theory and Experiment for Near-Surface Flight

Nature of Result: The Ram-Wing is an efficient high-speed surface effect vehicle. A simple flow model has been developed and its performance predictions corroborated by wind tunnel tests. Free flight models have been successfully demonstrated over solid surfaces. An advanced wind tunnel model has a measured lift/drag ratio of over 30.

Significance: The Ram-Wing can easily meet the cruise performance objectives of the ARPA surface effect vehicle program which calls for a gross weight of 1000 tons, speeds to 200 K, and a range of 4500 nm. Specifically, the research reported here can be used in preliminary design studies of ram-wing vehicles.

Possible Applications: The surface effect vehicle may be used in a variety of military missions described in Surface Effect Vehicle Summer Study. (ARPA Symposium 21 July – 15 August, 1969, Vols 1, 2, 3. ARPA No. S.349). A Ram-Wing vehicle (with appropriate modification for sea sitting and ice sitting) should be considered for the ARPA surface effect vehicle program.

RA FJSRL 70-9

Contact: Captain Roger W. Gallington, FJSRL/NA
Telephone Ext. 3121

Research Needs

State-of-Charge Level Sensing in Secondary Batteries

Problem: A method is needed for determining the state-of-charge (within ±5% of the deliverable ampere-hour capacity) of nickel cadmium, silver cadmium, and silver zinc batteries. In the past, a lack of information on the state-of-charge of the batteries has compromised spacecraft missions.

State-of-the-Art: No reliable and accurate method for determining the state-of-charge of alkaline batteries exists. Voltage measurements during pulse charges, integrating ampere-hour meters, coulometers (electrical charge meters), and impedance and capacitance measurement techniques have been investigated with only limited success. Although methods for signaling full charge have been developed, there is no reliable technique to indicate state-of-charge between zero and full charge.

Background: State-of-charge indicators have been investigated by AFAPL, the Army, Navy, and NASA with only limited success. Within very restricted temperatures, various methods have shown promise of determining load power profile and cycle life regimes. These techniques have all been inadequate or impractical, however, when applied over the electrical and operating environments experienced in flight vehicle battery applications. At present, AFAPL has no active efforts in support of this requirement; basic research is needed for innovative approaches.

References:

(1) Army 18th and 19th Annual Power Sources Conference Proceedings
(2) AEC Health and Safety Laboratory Report HASL-198.

Project No. 3145 RN AFAPL-71-21

Contact: R.L. Kerr, AFAPL/POE-1
Telephone Ext. 52435

Boiling Phenomena Associated with Confined Spaces

Problem: With the advent of integrated circuit technology and miniaturization of electronic components, heat generation rates have increased significantly. Computers and many other electronic systems using solid state devices operate with heat fluxes of about 2 watts/in^2, still within the capability of forced air cooling. More recently developed equipment, however, will generate heat fluxes up to 200 watts/in^2 and even higher. For such heat fluxes, the most effective mode of heat transfer is evaporation.

State-of-the-Art:

(a) Pool and forced convection boiling from ordinary surfaces have been studied by many investigators, providing both analytical and experimental data. Studies are needed, however, to investigate both the dynamic and the thermal behavior of nucleate boiling on very small heat transfer surfaces whose dimensions are of the same order of magnitude as the detaching bubbles, or even smaller.

(b) Recent developments in application of heat pipes in electronic equipment cooling have created a need for predicting both boiling and condensing heat transfer coefficients from wick covered heat transfer surfaces. Boiling in wicks is a complicated phenomenon about which limited data are available, particularly concerning fluids with low boiling temperatures (room temperature or thereabouts). A recent study examined the mechanism of vaporization heat transfer on a system with a fluid-wick combination that had well-defined geometric parameters (beds of packed beads) and physical properties. However, data on vaporization heat transfer from surfaces covered with ordinary wicks are limited.

Background: Heat transfer may limit the size of microelectronic cooling devices unless means for achieving higher boiling heat transfer rates can be achieved. Two-phase devices such as the heat pipe are gaining in application for both aircraft and spacecraft systems, but their development is sometimes hampered by a lack of fundamental theory necessary to properly design boiling and condensing surfaces.

References:

(1) Bergees, A.E., N. Bakkru, and J.W. Shires, "Cooling of High-Power Density Computer Components," *MIT Report No. DSR 70712-60.*
(2) Allingham, W.D., and J.A. McEntire, "Determination of Boiling Film Coefficient for a Heated Horizontal Tube in Water-Saturated Wick Material," *ASME Paper No. 60-HT-11,* September 1960.
(3) Ferrell, J.K. et al., "A Study of the Operating Characteristics of the Heat Pipe," *North Carolina State University Report No. ORO-3411-12,* Part 3, April 1969.

Project No. 6146 RN AFFDL 71-16

Contact: C.J. Feldmanis, AFFDL/FEE
Telephone Ext. 3021

MHD Lasers

Problem: To determine the possibility of creating laser action through the interaction of a conducting fluid moving through a magnetic field. An ionized inert gas MHD generator can heat the electrons to temperatures well above the gas or ion temperature and above the gas stagnation temperature through self-induced ohmic heating current. Basically, the MHD generator has the physical ingredients for internally combining the process of converting thermal to electrical power with the process of converting electrical to radiative power. There are no moving hardware parts. Eliminating one coupling step reduces power loss in the transfer from one type of converter to the other. Significant weight reduction may also result.

State-of-the-Art: MHD experiments and analysis have shown that a population inversion in inert and combustion gases may be created in the MHD channel.

Background: Analysis has emphasized the CO_2, 10.6 micron system; other laser systems need to be analyzed.

Reference: Final report *Contract F33615-69-C-1450,* "Research on MHD Energy Conversion," now in print.

Project No. 3145 RN AFAPL-71-27

Contact: Paul D. Lindquist, AFAPL/POP-2
Telephone Ext. 53036

Type II Superconductors and Their Applications

Problem: To improve Type II superconductors and their utilization in high field lightweight magnets for MHD (magnetohydrodynamics), inductive energy storage, and rotating machinery.

State-of-the-Art:

(a) Superconductors: Copper stabilized Nb-Ti and Nb_3Sn can now be had for use in steady state magnets (i.e., MHD). Nb_3Sn has a high field capability, but is obtainable only in tape that is difficult to wind into other than solenoidal shapes. Nb-Ti is available as wires of various cross-sections. Aluminum stabilization of these superconductors, which has been achieved only by using an intermediate copper layer, could reduce the weight and increase the current density of future systems.

For inductive energy storage and rotating machinery, the superconductor must be able to operate under transients (electromagnetic and/or mechanical). The theory for designing appropriate superconducting conductors, and some experimental results, are available. However, fabrication of these conductors for large transient-operation devices has not yet been accomplished.

(b) MHD Magnets: A 4500-pound saddle-shaped magnet, built by Airco Temescal, has achieved 3.3 tesla in a 7-inch bore in preliminary tests. Two lightweight MHD magnets (4.0 tesla, 10-inch bore, 1000 pounds; and 5.0 tesla, 7-inch bore, 1000 pounds), presently in development, are scheduled for completion in 1971 and 1972, respectively.

(c) Inductive Energy Storage: A large heavy device, built by AVCO-Everett and operated successfully, delivered 86 kilojoules to a load in a 4-millisecond pulse duration. For higher energy level, shorter pulse duration, lighter weight devices, current interruption switching becomes a difficult problem.

(d) Rotating Machinery: An 80 kva machine, built at M.I.T., proves that liquid helium can be used successfully in a rotating dewar vessel to cool a superconducting field winding. This machine's specific weight is 3.75 pounds per kva. Higher speed, higher magnetic field designs promise orders of magnitude reduction in specific weight.

Background: These applications of Type II superconductors are directed toward producing high power for U.S. Air Force applications such as lasers, ECM, OCM, and photoreconnaissance.

References:

(1) Magnets: Contracts F33615-69-C-1212; F33615-70-1567; AFAPL TR-69-119
(2) Inductive Energy Storage: AFAPL TR-69-101; AFAPL-TR-69-102
(3) Rotating Machinery: Thulen, et al, IEEE Power Group, September 1969.

Project No. 3145 RN AFAPL-71-30

Contact: Ronald Pape, AFAPL/APIE-2
Telephone Ext. 53036

Fracture Mechanics—Crack Stoppers

Problem: High strength materials and, in particular, high strength materials with low fracture toughness are extremely sensitive to small flaws or minute amounts of damage. Unfortunately, when such materials are used in an airframe, it is possible for small, nondetectable flaws to propagate to a length at which catastrophic failure can occur in the time between inspection cycles.

State-of-the-Art: A method, commonly used on thin sheet aluminum structures for slowing and/or stopping the propagation of a crack, consists of blunting the tip of the crack—lowering the stress at the tip—by drilling a hole at the end of the crack. For thicker sections and higher strength materials, this procedure is not practical.

Background: Great emphasis has been placed upon fracture mechanics theory and damage tolerant structural design as the direct result of the catastrophic inflight failure of the wing of F-111 Airplane No. 94 (AFSN 67-049) in December 1969 and of the problems that developed from the cracking of the F-100 and C-130 wing skins. Therefore, an

effective means for slowing and/or stopping the growth of flaws or cracks in high strength materials must be investigated. One suggested means would involve the reduction of the ultimate tensile strength, by thermal means, with an accompanying increase in fracture toughness in a very localized zone across the tip of the crack. Another suggested method involves the establishment of compressive stresses, by mechanical or electromagnetic means, around the tip of the crack.

Project No. 1467 RN AFFDL-71-19

Contact: R.F. Hoener, AFFDL/FB
Telephone Ext. 5723

Data Signaling Above Nyquist Rate

Problem: Basic research in high speed data transmission is required to exploit the possibility of data signaling above the Nyquist rate through application of adaptive decision directed feedback techniques.

State-of-the-Art: Available linear devices, which include transversal equalizers and linear modulation-demodulation techniques, cannot support data signaling rates above the Nyquist rate. In practical implementations, any linear device that would adequately reduce intersymbol interference when signalizing above the Nyquist rate would greatly reduce the effective signal-to-noise ratio. This would result in below optimum performance because of greater amplification of noise than of the desired signal.

Background: In his classical works, Nyquist proved that data cannot be transmitted reliably at a symbol rate higher than twice the total bandwidth when utilizing linear devices. However, considerable promise exists for eliminating this signaling boundary by resorting to nonlinear techniques in the receiver design. Reference (2) outlines work and simulations already done, and accents the possibilities of this technique.

References:

(1) Nyquist, H., "Certain Topics in Telegraph Transmission Theory," *Transactions of the AIEE*, Vol 47 (April 1925) 617-644
(2) Bowen, R.R., D.A. George, and J.R. Storey, "An Adaptive Decision Feedback Equalizer," Conference Record, *1970 International Conference on Communication*, Vol I (Jun 70) 16-24

Project No. 6523 RN RADC-71-4

Contact: George E. Carter, RADC/COAD
Telephone Ext. 2859

Area Ratio Ejectors As STOL High Lift and Propulsion Devices

Problem: Wind tunnel model tests are required to provide basic data on the performance and aerodynamic characteristics of a combination STOL high lift wing/propulsion concept employing a low area ratio thrust augmentation ejector.

State-of-the-Art: Preliminary performance calculations for low area ratio ejectors have been made by ASD, using a theory developed at ARL; however, experimental confirmation of this theory has not been accomplished. There are currently no proven theoretical or empirical methods for computing the aerodynamic or propulsion characteristics of such devices in the take-off, climb, cruise, and landing flight regimes.

Background: The ARL has for several years been supporting an active research program in the area of thrust augmenting ejectors, with emphasis on potential application to vertical take-off and landing (VTOL) aircraft. Recently, based on ASD studies, interest has shifted to include the short take-off and landing (STOL) aircraft concepts. The experimental data developed to date by ARL does not apply to the STOL configurations of interest within ASD because of significant geometric differences and vastly different operational modes. The VTOL applications require large area ratio ejectors optimized for high static thrust. The concept, developed by ARL and ASD for the STOL aircraft, employs low area ratio ejectors, optimized for operation throughout the aircraft flight regime. In the take-off regime, the ejector performs identically to the NASA Ames/de Havilland "Augmented Jet Flap"; however, the de Havilland concept is retracted into the trailing edge of the wing and is not operational above the flaps up airspeed of the aircraft.

The unique aspects of a high lift ejector system, used as a forward propulsion system, have not been previously investigated. Little information exists on low area ratio ejectors, and none of the configurations previously investigated were fashioned in a spanwise, integrated propulsive wing system such as proposed. The high speed potential of this concept has not been determined.

References:

(1) "Design Techniques for Prediction of the Aerodynamic Characteristics of STOL Aircraft Using Ejector Augmented Blown Flaps," *TN-ASD-71-108.*
(2) Cook, A.M., et al., "Low Speed Aerodynamic Characteristics of a Large Scale STOL Transport Model With an Augmented Jet Flap," *NASA Working Paper 251.*

Project No. 1366 RN AFFDL-71-18

Contact: Rodney L. Clark, AFFDL/FXM
Telephone Ext. 52786

Speech Digitization Techniques

Problem: Research is needed in the area of speech processing and digitization to develop more efficient bandwidth techniques for both secure and non-secure digital speech communications.

State-of-the-Art: Voice digitization techniques, which offer speech intelligibility and naturalness comparable to that achieved on good analog voice channels, currently require data rates between 38.4 and 64 kilobits per second. These devices use various forms of pulse code modulation and delta modulation to convert the voice signal to a digital form.

Background: A number of techniques, including continuous variable slope delta modulation at 19.2 kilobits per second and voice excited vocoders at 9.6 kilobits per second, offer suitable intelligibility at data rates well below 38.4 kilobits per second; however, these techniques leave much to be desired in naturalness or speaker recognition.

References:

(1) MALLARD System Report, *Sylvania Electronic Systems TR-5* Vol 2B, ECOM-0120-5, pages 26-104.
(2) "Comparative Testing of Voice Digitizers and Modes," *Communications and Systems, Inc.*, 24 Apr 1969, DCA Contract 100-69-0009.

Project No. 6523 RN RADC-71-5

Contact: William D. Alexander, RADC/COAD
Telephone Ext. 2859

Hundred Megabit to Gigabit Logic Study

Problem: A need exists to develop integrated circuit devices which can operate properly with minimal power consumption at the hundred megabit to gigabit rates over the full Mil-Std temperature range.

State-of-the-Art: Some presently off-the-shelf circuits are capable of switching at speeds of approximately 350 megabit/sec. These devices use Emitter Coupled Logic to perform necessary gating and storage. Some higher rates have been achieved on in-house experimental devices, but no standard military communication equipment using such high speed circuits has been produced. The power consumption of the 350 megabit MECL III logic is rather high, approximately 55 mW per gate.

Background: In recent years, digital data traffic over communication channels has increased substantially. There has also been a significant increase in rates. Digital color and black and white television, as well as certain computer terminals, operate at a tens-of-megabits rate. For efficient transmission of this data traffic, switching and multiplexing become a system requirement. When such high rate channels are combined to produce even higher rates, logic speed and internal propagation delay times become severe problems. Frequently, circuits operating at high speed can be used only in controlled temperature environments. The full Mil-Std temperature range makes the production and operation of the high speed elements more difficult. Power consumption of these devices would become prohibitive if implemented in an equipment such as a multiplexer.

References: For further background and study, the semi-conductor divisions of Motorola, Fairchild, Texas Instruments, and Raytheon Corporation are suggested.

Project No. 6523 RN RADC-71-7

Contact: Ronald L. Torezan, RADC/COAT
Telephone Ext. 7000

1971 Index of Air Force Research Review

Key:	J/F	January-February	Number 1
	M/A	March-April	Number 2
	M/D	May-December	Number 3

Part I. By Title 32

Articles 32

Scientific Notes 33

Readers Interchange 34

- **Invention Disclosures** 34
- **Research Advances** 34
- **Research Needs** 34
- **Speculative Ideas** 35

Part II. By Author By-Line 35

Part III. By Sponsoring Organization 36

Part I. By Title

Articles

Aircraft Wakes: A New Look at a Classical Problem	J/F-4
Aluminum High Energy Density Concentration Cells	M/D-8
Approximation Theory	M/D-17
Flow Separation on a Slender Cone at Angle of Attack	M/D-4
Human Resources Data in System Analysis and Design	J/F-9
Inertial Navigation, Guidance, & Control Research	M/D-14
Measurements of Surface Irregularities and Spin Dynamics of the PAGEOS Balloon-Satellite by Photoelectric Photometry	J/F-13
A Novel Electro-Optical Rotation Sensor	J/F-8
Regularizable Ill-Posed Problems	M/D-1
Rotating Flows	J/F-1
Time Series Analysis and Statistical Meteorology	J/F-17
X-Ray Photographs of Powder in Vortex Flows	M/D-12

Scientific Notes

Compressive Behavior of Unidirectional Fiber Reinforced Plastic Composites	M/D-21
Design and Synthesis of Materials Lasers	M/A-15
Erosion Mechanisms of Graphite Materials	M/D-21
Fracture Mechanics of Fiber Reinforced Laminated Plastic Composites	M/D-19
Geodetic Application of Long Base Interferometry	M/A-15
High Resolution Chemical Ionization Mass Spectroscopy	M/A-14
Irradiation Defects and the Electrical Quality of Ion Implanted Silicon	M/A-14
Laser Research	M/A-13
Low Temperature Infrared Spectroscopy of Hydrogen Bonded Polymers	M/D-20
Mass Spectrometric Determination of Volatile Electrode Products	M/D-20
A Model for Evaluating the Utility of Forecasting Natural Environmental Phenomena	M/A-15
New, Improved Shift Reagents for Simplifying NMR Spectra	M/D-22
A New Vacuum Microbalance Space Physics Laboratory	M/A-12
Oxidation of Titanium-Aluminum-Gallium Alloys	M/D-19
Rare Earth Cobalt Magnets	M/A-12
Studies to Improve Radar Target Perception	M/D-20
Supersonic Turns Without Superbooms	M/D-20
Vuilleumier Cycle Cryogenic Coolers Demonstrate a New Era in Aircraft Reliability	M/A-13
Yttrium Orthoaluminate—An Important New Laser Host Material	M/D-22

Readers Interchange

Invention Disclosures

Boundary Layer Probe	M/D-24
Deflection Modulation Display	M/D-24
Electrogasdynamic Generator Method and Apparatus	J/F-25
Electro-Pneumatic Servo Flowmeter	J/F-25
Epoxy Resistance Thermometer	M/D-24
Improved NMR Probe for Magnetic Field Measurements	M/D-24
Method of Fabricating Lightweight Targets for Radar Measurements	M/D-24
A Method of Measuring the Pressure Dependence of the Thermal Conductivity of Gases	J/F-25
New Propyl OOF Isomers	J/F-25
Self-Activating Recording Gage	J/F-26
Submillimeter Frequency Measuring System	J/F-26
Transfer Discharge Ion Getter Vacuum Pump	M/D-24
Transient Data Recorder	J/F-26
A Wideband, Low Noise Frequency Modulator That Can Be Used for Rapid Modulating Rates	M/D-24

Research Advances

Catalyst for Gaseous Hydrocarbon Reactions	M/A-17
Configuration Optimization of a Class of Hypersonic Cruise Vehicles	M/A-17
Effect of Unsymmetrical Nose-Bluntness on Stability Derivatives	M/D-25
Electrofluid Dynamic Energy Conversion	M/A-17
Exoatmospheric Infrared Calibration	M/D-25
Langmuir Probe Data Reduction Program	M/D-25
Model for a Short-Range Dogfight Missile	M/D-26
New Centrifuge Test Method for Inertial Gyroscopes	M/D-26
Optical Probing Data Reduction Program	M/A-18
Oxidation of Ni-Base Alloys Containing Additions of Cr, Al, and/or Y	M/A-18
Passive Optical Techniques for Space Object and Target Identification	M/D-25
The Ram-Wing: Theory and Experiment for Near-Surface Flight	M/D-26
Transient Analysis and Optimal Design of Nonlinear Dynamic Circuits	M/A-17
Type Conversion by Ion Implantation	M/A-18

Research Needs

Aeromedical Assessment of Phase Dilution Aviator's Oxygen Concept	M/A-19
Area Ratio Ejectors As STOL High Lift and Propulsion Devices	M/D-29
Automated Mesh Generation Techniques for Structural Shell Analysis	M/A-20
Boiling Phenomena Associated With Confined Spaces	M/D-27
Combustion Processes in Airbreathing Engines	M/A-22
Data Signaling Above Nyquist Rate	M/D-29
Fracture Mechanics—Crack Stoppers	M/D-28
Fracture Mechanics of Advanced Filamentary Composite Structures	M/A-20
Fundamental Parameters Affecting Foaming Characteristics of Lubricants	M/A-24
Higher Efficiency Solar Cells Through Improvements in the Silicon Starting Material	M/A-21
High Energy Density Electrochemical Power Sources for Electronic Countermeasure Devices	M/A-22
High Energy Endothermic Chemical-Kinetic Reactions for Use as Long Term Heat Sinks	M/A-20
Hundred Megabit to Gigabit Logic Study	M/D-30
Improved Lubricant Pumpability at Low Temperatures	M/A-23
Infrared Measurements of Aerodynamic Heating	M/A-19
Low Cost Fuel Cell Electrodes for Operation on Propellant Grade Reactants	M/A-22

Research Needs (continued)

Method of Correlating the Wake Shape of a Statically Operating Propeller or Rotor with Readily Available Blade Geometry Data M/A-21
MHD Lasers M/D-28
Power Flow Coupling Coefficients for Statistical Energy Analysis of Vibrating Systems M/A-19
Prediction of Near Field Noise of Supersonic Jets M/A-23
Speech Digitization Techniques M/D-30
State-of-Charge Level Sensing in Secondary Batteries M/D-27
Transonic Unsteady Aerodynamic Prediction Method M/A-20
Type II Superconductors and Their Applications M/D-28

Speculative Ideas
Method for Shock Wave Modification J/F-23
New Shape of a Reentry Body J/F-24
Test Criteria To Predict the Degradation of Manned Weapons Systems During Combat J/F-23

Part II. Author By-Line

Askren, William B., Dr. J/F-9

Carr, Paul H. M/A-6

DeVito, Peter A. M/A-6

Fannin, Armand A., Jr., Capt M/D-8
Finkleman, David, Capt M/A-1

Gleser, Leon J., Dr. J/F-17

Hasinger, Siegfried H. J/F-1
Hyde, John Paul, Lt Col M/D-14

Kearns, William J. M/A-6
King, Lowell A., Lt Col M/D-8

Lee, David A., Dr. M/D-1

Mailloux, Robert J., Dr. M/A-4

Newburgh, R.G., Dr. J/F-8

Phipps, T.E., Jr., Dr. J/F-8

Seegmiller, David W. M/D-8
Shields, W.L., Col J/F-4
Shisha, O., Dr. M/D-17
Silva, Jose H., Jr. M/A-6
Stetson, Kenneth F. M/D-4

Turman, B.N., Lt M/D-12
Trott, William R., Lt Col J/F-17

Vanderburgh, Richard C. J/F-13

Part III. Sponsoring Organization

Aerospace Research Laboratories	
Applied Mathematics Research Laboratory	M/D-1
Energy Conversion Research Laboratory	J/F-1, M/D-12
Fluid Dynamics Facilities Research Laboratory	M/D-4
General Physics Research Laboratory	J/F-13
Air Force Cambridge Research Laboratories	
Microwave Physics Laboratory	J/F-8, M/A-4, M/A-6
Air Force Human Resources Laboratory	
Advanced Systems Division	J/F-9
Air Force Office of Scientific Research	
Directorate of Mathematical and Information Sciences	J/F-17
The Frank J. Seiler Research Laboratory	
Directorate of Aerospace-Mechanics Sciences	M/A-1, M/D-14
Johns Hopkins University	J/F-17
Naval Ordnance Laboratory	J/F-8
U.S. Air Force Academy	
Department of Chemistry	M/D-8

GPO 920-526

AFSC LABORATORIES

Aerospace Research Laboratories (ARL)
6570 Aerospace Medical Research Laboratory (AMRL)
Air Force Aero Propulsion Laboratory (AFAPL)
Air Force Avionics Laboratory (AFAL)
Air Force Flight Dynamics Laboratory (AFFDL)
Air Force Materials Laboratory (AFML)
Wright-Patterson AFB, Ohio 45433
Telephone: Area Code 513 - 25 + xxxxx
AUTOVON 78 + xxxxx

Air Force Armament Laboratory (AFATL)
Eglin AFB, Florida 32542
Telephone: Area Code 904 - 882 + xxxx
AUTOVON 872 + xxxx

Air Force Cambridge Research Laboratories (AFCRL)
L.G. Hanscom Field, Bedford, Massachusetts 01730
Telephone: Area Code 617 - 861 + xxxx
AUTOVON 478 + xxxx

Air Force Human Resources Laboratory (AFHRL)
Brooks AFB, Texas 78235
Telephone: Area Code 512 - 536 + xxxx
AUTOVON 240 + xxxx

Air Force Office of Scientific Research (AFOSR)
1400 Wilson Boulevard, Arlington, Virginia 22209
Telephone: Area Code 202 - 69 + xxxxx
AUTOVON 22 + xxxxx

Air Force Rocket Propulsion Laboratory (AFRPL)
Edwards AFB, California 93523
Telephone: Area Code 805 - 277 + xxxx
AUTOVON 350 + xxxx

Air Force Weapons Laboratory (AFWL)
Kirtland AFB, New Mexico 87117
Telephone: Area Code 505 - 247 + xxxx
AUTOVON 946 + xxxx

Rome Air Development Center (RADC)
Griffiss AFB, New York 13440
Telephone: Area Code 315 - 330 + xxxx
AUTOVON 587 + xxxx

The Frank J. Seiler Research Laboratory (FJSRL)
USAF Academy, Colorado 80840
Telephone: Area Code 303 - 472 + xxxx
AUTOVON 259 + xxxx

AFSC/DLLT
Andrews Air Force Base
Washington, D.C. 20331

UNITED STATES AIR FORCE
OFFICIAL BUSINESS

POSTAGE AND FEES PAID
DEPARTMENT OF THE AIR FORCE